doi : 10.17596/0003234

KAIREI Cruise Report

KR08-10

Studies on the thermal structure and the water distribution in the upper part of the Pacific plate subducting along the Japan Trench

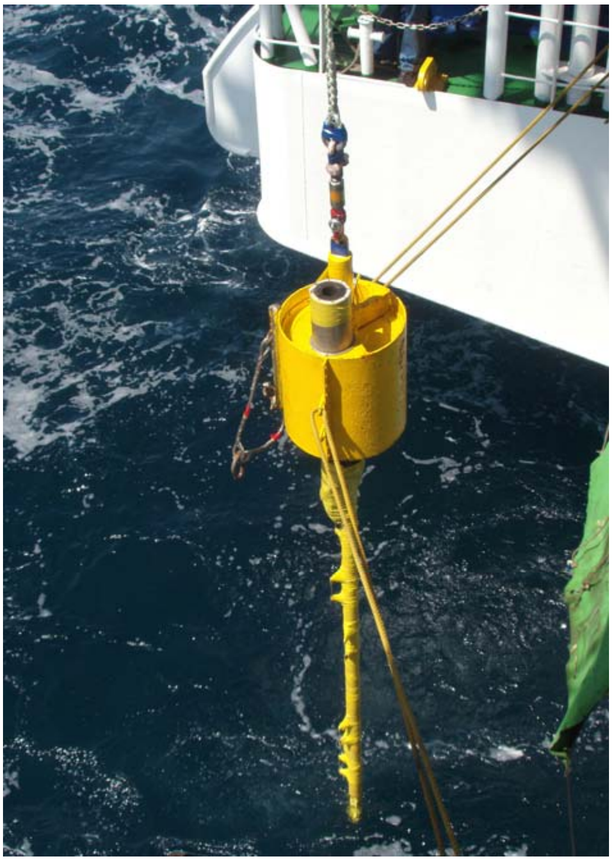

Japan Trench area

August 18, 2008 – September 11, 2008

Japan Agency for Marine-Earth Science and Technology
(JAMSTEC)

Contents

1. Cruise Information

Cruise number:

KR08-10

Ship name:

R/V KAIREI (with ROV KAIKO 7000II)

Title of the cruise:

2008 Deep Sea Research

Research cruise with KAIREI and research dives with KAIKO 7000II

Title of proposal:

S08-66

Studies on the thermal structure and the water distribution in the upper part of the Pacific plate subducting along the Japan Trench

Cruise period:

August 18, 2008 – September 11, 2008

Port call:

2008 Aug. 18	Dept. from Yokosuka (JAMSTEC)
Sep. 1	Arriv. at Miyako
Sep. 2	Dept. from Miyako
Sep. 10	Arriv. at Yokosuka (JAMSTEC)

Research area:

Japan Trench area

Research map:

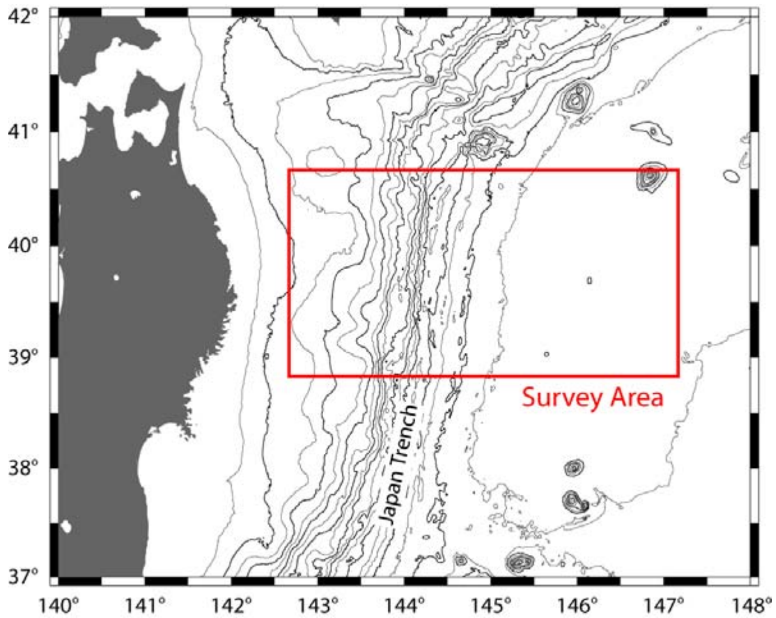

Figure 1-1. Survey area of KR08-10 cruise.

Ship track and observation points are shown in 3.2.3.

2. Researchers

Chief Scientist:

Makoto YAMANO	Earthquake Research Institute, University of Tokyo

Deputy Chief Scientist (Leg 2):

Tada-nori GOTO	Institute for Research on Earth Evolution (IFREE), JAMSTEC

Science Party:

Makoto YAMANO	Earthquake Research Institute, University of Tokyo	(Leg 1)
Tada-nori GOTO	IFREE, JAMSTEC	(Legs 1, 2)
Kiichiro KAWAMURA	Fukada Geological Institute	(Legs 1, 2)
Hideki HAMAMOTO	Earthquake Research Institute, University of Tokyo	(Legs 1, 2)
Kiyoshi BABA	Earthquake Research Institute, University of Tokyo	(Leg 2)
Makoto HARADA	Institute of Oceanic Research and Development, Tokai University	(Leg 2)
Tomoko HANYU	Department of Polar Science, The Graduate University for Advanced Studies	(Leg 2)
Yoshifumi KAWADA	IFREE, JAMSTEC	(Leg 2)
Noriaki SAKURAI	IFREE, JAMSTEC Facalty of Ocean Research, Tokai University	(Leg 2)
Masataka KINOSHITA	IFREE, JAMSTEC	(shore-based)
Shusaku GOTO	Institute for Geo-Resources and Environment, National Institute of Advanced Industrial Science and Technology	(shore-based)
Keiko FUJINO	Graduate School of Engineering, Kyushu University	(shore-based)
Tetsuzo SENO	Earthquake Research Institute, University of Tokyo	(shore-based)
Junji YAMAMOTO	Institute for Geothermal Sciences, Kyoto University	(shore-based)
Yuka MASAKI	IFREE, JAMSTEC Graduate School of Science, Kochi University	(shore-based)
Toshiya FUJIWARA	IFREE, JAMSTEC	(shore-based)

Technical Support Staff

Satomi MINAMIZAWA	Nippon Marine Enterprises, Ltd.	(Legs 1, 2)
Ei. HATAKEYAMA	Marine Works Japan, Ltd.	(Legs 1, 2)
Naotaka. TOGASHI	Marine Works Japan, Ltd.	(Legs 1, 2)
Akira. SO	Marine Works Japan, Ltd.	(Legs 1, 2)

3. Observation

3.1. Introduction

In the Japan Trench subduction zone, an old oceanic plate with an age of over 100 m.y., the Pacific plate, is subducting beneath the northeast Japan arc. Recent studies have revealed that the Pacific plate just before subduction may not be uniformly cold contrary to its old age.

Yamano et al. (2008) conducted heat flow measurements on the seaward slope and the outer rise of the Japan Trench along a parallel of 38°45'N and showed the existence of high heat flow anomalies (Fig. 3.1.1). High heat flow values (70 to 115 mW/m^2) were obtained at many stations, while values normal for the seafloor age (about 50 mW/m^2) were also observed at some stations. It suggests that thermal structure of the Pacific plate in this area is not a typical one for old oceanic lithosphere, at least at shallow depths.

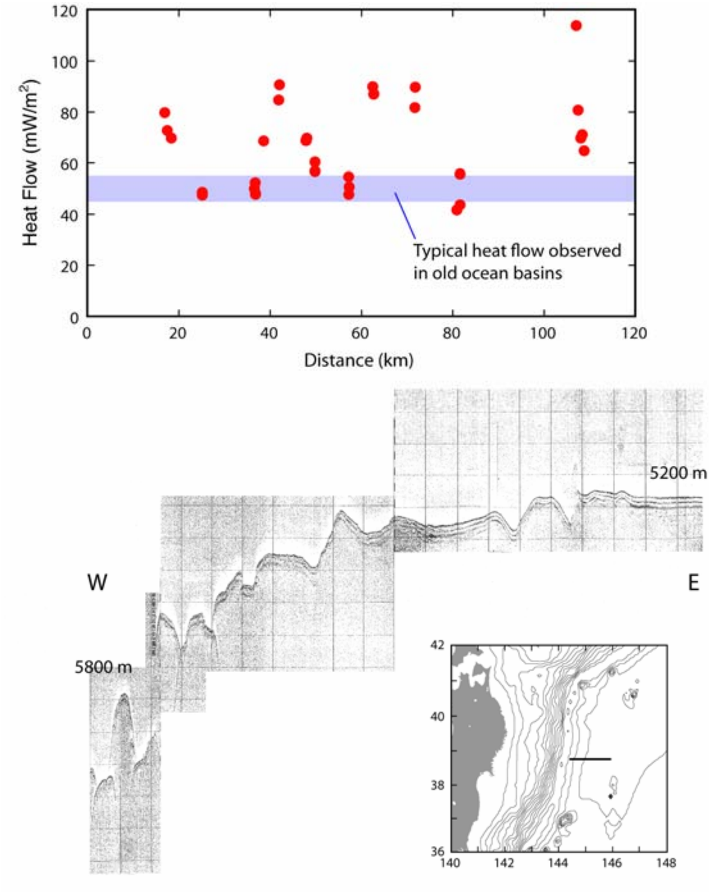

Figure 3.1-1. Heat flow profile on the seaward slope of the Japan Trench along a parallel of 38°45'N projected on a 3.5 kHz subbottom profiler record (Yamano et al., 2008).

Another recent finding is a peculiar type of intra-plate volcanism around the outer rise of the Japan Trench, which is called “petit spot” (Hirano et al., 2001; 2006). Basaltic rocks with radiometric ages ranging from 4.2 to 8.5 m.y. were collected on the seaward slope of the trench and even younger rocks (younger than 1 m.y.) were found on the eastern edge of the outer rise. This volcanism might provide a heat source of the observed high heat flow anomalies and exert a significant influence on the thermal structure of the Pacific plate.

Subduction of oceanic plate causes large thrust earthquakes along the interface with the overlying landward plate. The extent of the seismogenic zone of these earthquakes is thought to be controlled mainly by the temperature distribution along the plate interface (e.g., Oleskevich et al., 1999). The existence of water along the plate interface should also play important roles in the stress accumulation and rupture processes in the seismogenic zone. In the Japan Trench subduction zone, the nature of the seismogenic zone, such as seismicity, size of asperities and coupling of the plates, significantly varies along the trench (e.g., Yamanaka and Kikuchi, 2004). Such variations could be related to the temperature structure and water content along the plate interface.

It is therefore important to accurately estimate the temperature structure around the plate interface for studies of seismogenic processes in the Japan Trench subduction zone. We, however, do not have surface heat flow data enough to constrain the thermal model of the subduction zone. It is necessary to conduct more systematic and dense heat flow measurements both on the seaward and landward slopes of the trench..

Results of electromagnetic survey conducted on the landward slope of the Japan Trench show that the subducted oceanic crust has high electrical conductivity and thus contains a large amount of water (Goto et al., 2001), though we do not know where and how the water penetrated into the crust. It is critically important to clarify the penetration process and distribution of the water in the oceanic crust for investigation of the mechanical properties of the plate interface.

3.2. Summary of the Cruise

3.2.1. Research items

(1) Heat flow measurement

Heat flow measurement with ordinary deep-sea heat flow probes and stand-alone heat flow meter (SAHF) designed for use in submersible dives.

(2) Long-term temperature monitoring on the seafloor

Long-term monitoring of the bottom water temperature and temperature profile in surface sediment using pop-up type instruments for determination of heat flow in areas with relatively shallow water depths.

(3) Piston core sampling with heat flow measurement (HFPC)

Sampling of surface sediments with a piston corer and heat flow measurement at the same site using temperature sensors mounted on the core barrel.

(4) Ocean-bottom electromagnetic survey

Controlled-source electromagnetic survey with KAIKO 7000II system and magnetotelluric survey with high-frequency ocean-bottom electromagnetometers (HF-OBEMs) and long-term OBEMs (LT-OBEMs).

(5) Bathymetry and geophysical survey

Bathymetry mapping with a multi narrow beam system, gravity measurement, and .measurements of total magnetic field and geomagnetic vector.

3.2.2. Cruise schedule and operations

Date	Events, Operations
Aug. 18	Leave Yokosuka
Aug. 19	Arrive in the survey area Bathymetry and geophysical survey
Aug. 20	Deployment of OBE and OBEM (OBE103 and OBEM101) Heat flow measurements (HF01) Bathymetry and geophysical survey
Aug. 21	Piston core sampling with heat flow measurement (HFPC01) Heat flow measurements (HF02) Bathymetry and geophysical survey
Aug. 22	Heat flow measurements (HF03 and HF04) Bathymetry and geophysical survey
Aug. 23	Piston core sampling with heat flow measurement (HFPC02) Heat flow measurements (HF05) Deployment of OBE (OBE102)
Aug. 24	Bathymetry survey Heat flow measurements (HF06) Calibration test of pop-up long-term heat flow instrument Take refuge from rough sea (Miyako)
Aug. 25	Wait for the weather to improve (Miyako)
Aug. 26	Leave Miyako and arrive in the research area Bathymetry survey Heat flow measurements (HF07) Deployment of pop-up long-term heat flow instrument (PHF01) Deployment of pop-up water temperature monitoring system (PWT01) Calibration test of pop-up long-term heat flow instrument
Aug. 27	Piston core sampling with heat flow measurement (HFPC03) Heat flow measurements (HF08) Bathymetry and geophysical survey
Aug. 28	Heat flow measurements (HF09 and HF10) Bathymetry and geophysical survey
Aug. 29	Heat flow measurements (HF11) Bathymetry survey
Aug. 30	Heat flow measurements (HF12)

	Deployment of pop-up long-term heat flow instrument (PHF02) Piston core sampling with heat flow measurement (HFPC04) Bathymetry and geophysical survey
Aug. 31	Recovery of pop-up water temperature monitoring system (PWT02) Deployment of pop-up water temperature monitoring system (PWT03) Bathymetry survey Heat flow measurements (HF13) Leave the survey area
Sep. 1	Arrive at Miyako
Sep. 2	Leave Miyako Operation test of electric current source with KAIKO 7000II (Dive #428)
Sep. 3	Recovery of OBEM (OBEM101) Controlled-source electromagnetic survey with KAIKO 7000II (Dive #429) Bathymetry survey
Sep. 4	Recovery of two OBEs (OBE102 and OBE103) Heat flow measurements and core sampling with KAIKO 7000II (Dive #430) Bathymetry survey
Sep. 5	Sheave exchange off Miyako port Deployment of OBEM (L01) Bathymetry survey
Sep. 6	Piston core sampling with heat flow measurement (HFPC05) Bathymetry survey Heat flow measurements (HF14)
Sep. 7	Heat flow measurements (HF15)
Sep. 8	Deployment of OBEM (L02) Piston core sampling with heat flow measurement (HFPC06) Bathymetry survey
Sep. 9	Heat flow measurements (HF16) Bathymetry survey Leave the survey area
Sep. 10	Arrive at Yokosuka

Detailed cruise log is given in the Appendices (7-1).

3.2.3. Ship track and observation points

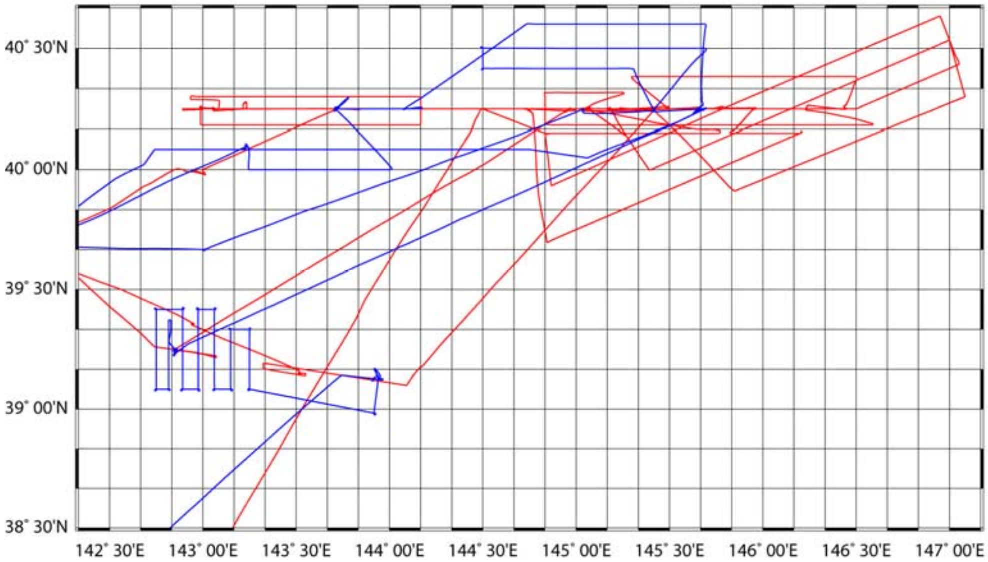

Figure 3.2-1. Ship track of KR08-10 cruise. Red and blue lines are track of Leg 1 and Leg 2 respectively.

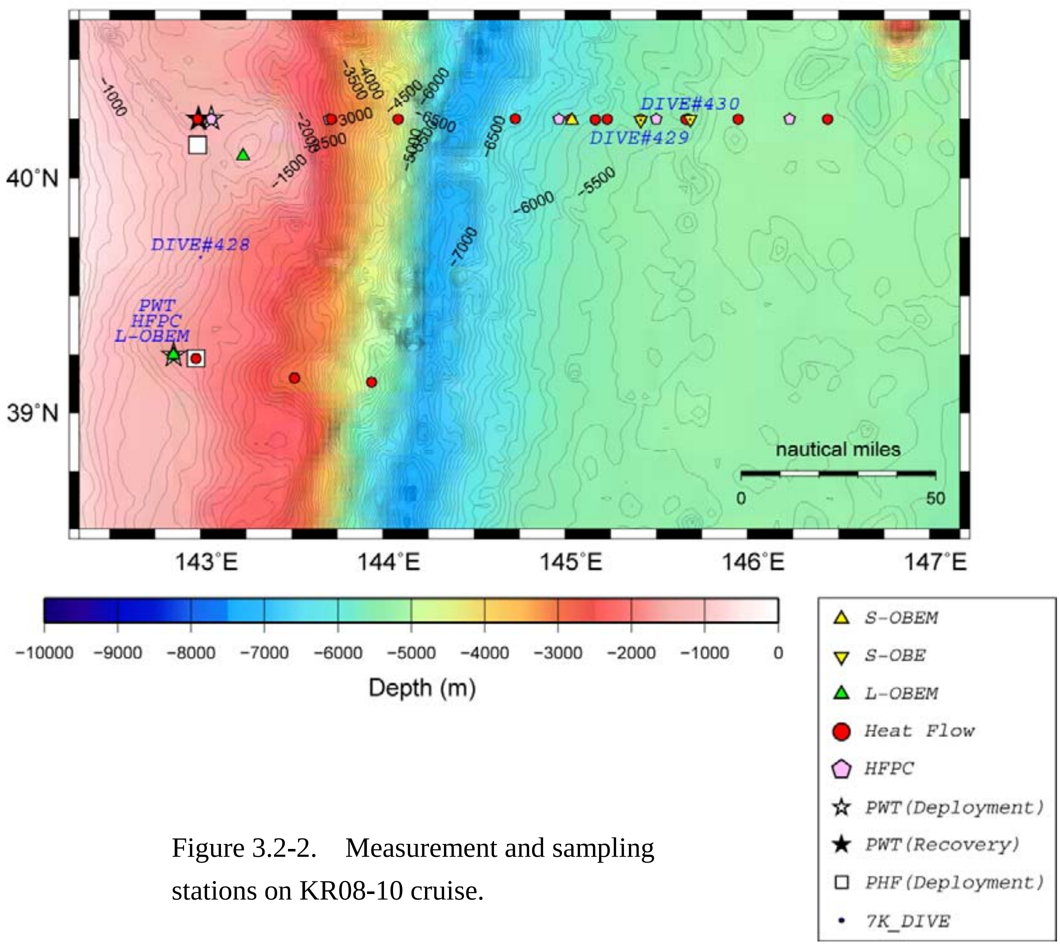

Figure 3.2-2. Measurement and sampling stations on KR08-10 cruise.

3.3. Research Objectives

We intend to clarify the temperature structure and the water distribution in the upper part of the Pacific plate subducting beneath the northeast Japan arc through heat flow measurements and electromagnetic surveys in the Japan Trench area. Based on the obtained results, we will investigate intra-plate volcanism on the Pacific plate, heat transfer and water movement in the oceanic crust associated with development of normal faults on the seaward slope of the Japan Trench. We also intend to examine relation between the temperature structure and water distribution along the subducting plate boundary and mechanical properties of the seismogenic zone.

3.3.1. Heat flow measurement

Heat flow values measured on the seaward slope of the Japan Trench along a parallel of 38°45'N are high at some locations and normal for the seafloor age at others (Yamano et al., 2008; Fig. 3.1-1). A possible cause of the spatial variation of heat flow is fluid flow along normal faults developed on the seaward slope of the trench, although no clear correlation between the heat flow distribution and the seafloor topography is recognized. The high average heat flow requires the existence of some heat source in the upper part of the plate. The heat source may be provided by intra-plate ("petit spot") volcanism taking place around the outer rise.

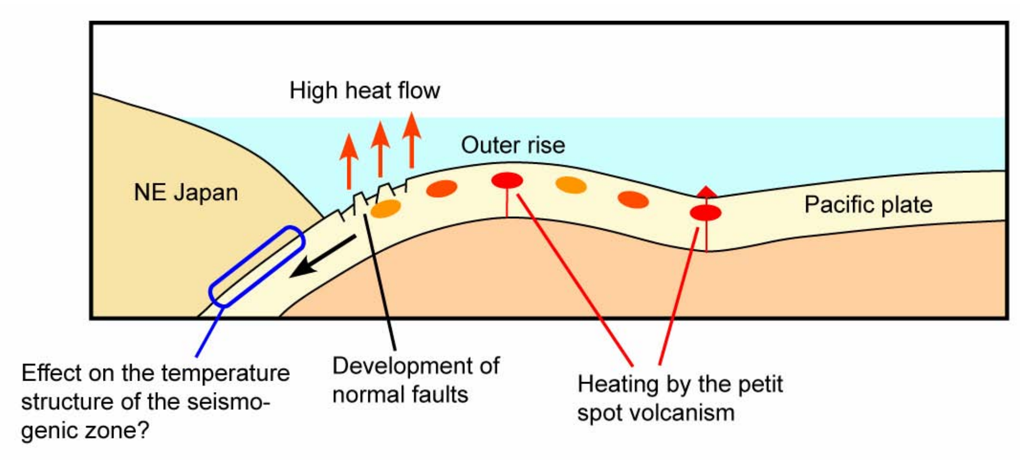

Figure 3.1-1. Schematic model of possible processes giving high heat flow on the seaward slope of the Japan Trench (Yamano et al., 2008).

A qualitative model which may account for the observed heat flow is shown in Fig. 3.3-1. When the Pacific plate reaches the trench outer rise area, melts due to the petit spot volcanism repeatedly intrude into the uppermost mantle and/or the lower crust with some eruption at the seafloor, and heat the surroundings. Then development of normal faults in the vicinity of the trench allows fluid flow along the fault zones, which carry heat and focus heat loss from the layers heated by intrusions. The effective vertical thermal diffusivity may vary from place to place depending on the permeability of fault zones and result in variable heat flow.

The above model presented above is rather speculative and needs to be improved through more geophysical and petrological studies, including detailed heat flow surveys. It is necessary to conduct measurements at different latitudes, to make dense measurements around sites with high values, and to investigate relationship between the heat flow distribution and the crustal structure. Such surveys need to be made on lines with seismic reflection data.

We chose a parallel of 40°15'N, along which a seismic refraction and reflection survey was conducted (Ito et al., 2004), as a survey line for detailed heat flow measurements. In 2007, we made preliminary measurements at three sites on the seaward trench slope on this line. Heat flow observed at two of the sites range from about 70 to 85 mW/m^2, indicating the existence of a anomaly similar to the one observed at 38°45'N. On this cruise, we carried out dense heat flow measurements on the seaward slope and outer rise along this survey line. Natural and controlled source electromagnetic surveys were also conducted on the same line (see 3.3.2).

The thermal structure of the subducting plate is one of the key factors which control the temperature distribution of the plate interface including the seismogenic zone of large thrust earthquakes. Subduction of the plate, the upper part of which has been anomalously heated, would result in an anomalous temperature structure in the seismogenic zone. It is important to estimate the subsurface thermal structure on the landward side of the trench as well in order to examine its relations to the thermal structure of the plate seaward of the trench and mechanical properties of the seismogenic zone. We therefore conducted heat flow measurements on the landward side of the trench along the 40°15'N line and at around 39°N.

3.3.2. Natural and controlled source electromagnetic survey

The Pacific plate at the seaward slope of the Japan Trench is very old and should have low heat flow values. However, recent dense heat flow measurements indicate high anomalies seaward of the Japan Trench (Yamano et al., 2008). In order to elucidate the source depth of high heat-flow anomalies, we conduct hybrid marine EM surveys with ocean-bottom electromagnetometers (OBEMs) in this cruise (Fig. 3.2-2).

We conduct three different ocean-bottom electromagnetic surveys around the Japan Trench as follows:

1) marine controlled-source electromagnetic (CSEM) survey with ROV Kaiko system,
2) marine magnetotelluric (MT) survey with short-term or high-frequency OBEMs (HF-OBEM) seaward of the Japan Trench,
3) marine MT survey with long-term OBEMs (LT-OBEMs) landward of the Japan Trench..

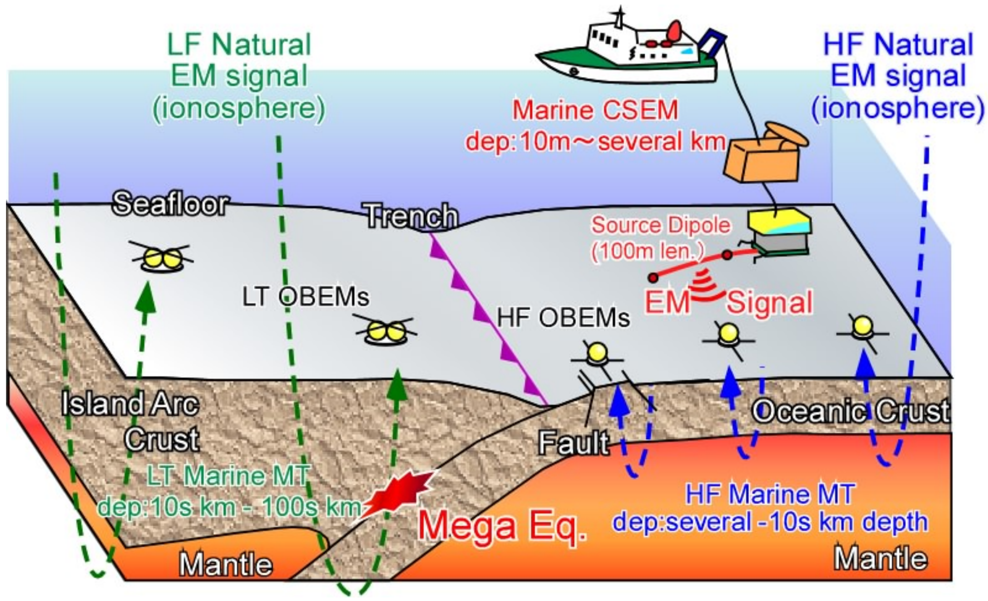

Figure 3.2-2. Basic concept of the hybrid marine EM survey on KR08-10 cruise.

Marine CSEM survey will image the electrical conductivity structure near the seafloor with depth of 10m – several km. We conduct marine CSEM surveys at two sites: near high heat-flow anomaly and normal areas. Marine MT surveys with HF-OBEMs can image the structure of crust and upper mantle with the depth range from several to several 10s km. We deploy three HF-OBE/OBEMs at the seaward slope. This combination of CSEM and MT surveys is effective to discuss the source depth of heat flow anomalies. For example, the oceanic crust with high fluid content and sub-seafloor groundwater circulation can yield both high heat flow and high electrical conductivity anomalies. High temperature zone below the seafloor can also yield high heat flow and conductivity anomalies. CSEM/MT surveys have possibility to detect the source depth of heat flow anomalies.

CSEM/MT surveys also elucidate how much fluid is included in the oceanic lithosphere of the Pacific plate before its subduction. Fluid in the oceanic lithosphere will be expelled below the Japan Arc after the subduction, relating to the earthquake occurrence near the Japan Trench. For example, Fujie et al. (2002) carried out seismic reflection survey in the Japan Trench region and found that large amplitude reflected waves generated at the subducting plate boundary were observed at low seismicity region and vice versa. The heterogeneous distribution of seismic reflectors may be attributed to heterogeneous fluid distribution on the plate boundary, and may indicate the role of fluid on the earthquake occurrences. However, we don’t know where the fluid is included in the oceanic lithosphere: at a ridge, fracture zones, hot spots or normal faults with horst/graben. Recently, Nakajima and Hasegawa (2006) found that a deep seismically active zone in the subducted Pacific plate corresponds to the elongated low seismic velocity zone, possibly interpreted as an old fracture zone with high fluid content. However, no observed results are reported relating to the fluid content in the oceanic lithosphere before the subduction.　In this cruise, we deploy two different types of OBEMs: three HF-OBE/OBEMs and two LT-OBEMs.　In addition, ten HF-OBEMs have been deployed and recovered at the landward slope of the Japan Trench in 2000.　Also, an LF-OBEM dataset was obtained at the outer rise of the Japan Trench in 2004.　Finally, we will obtain 13 HF-OBEM and 3 LT-OBEM datasets around the Japan Trench.　The dense and wide-band MT data give us the electrical conductivity structure of the oceanic lithosphere before and after subduction of the Pacific plate. Such an integrated electrical imaging allows us to discuss how much fluid is included around the normal faults in the horst and graben belt.

Finally, LT-OBEMs give us deeper mantle information.　During these several years, many LT-OBEMs have been deployed and recovered around Japan.　The long-term EM fluctuations obtained by the LT-OBEM array allow us to construct a regional 3-D mantle conductivity structure around Japan.　Two LT-OBEMs deployed landward of the Japan Trench in this cruise are important to image the forearc mantle and the subducting oceanic mantle structures.

3.4. Instruments and Operation Methods

3.4.1. Deep-sea heat flow probe

Heat flow is obtained as the product of the geothermal gradient and the thermal conductivity. We measured the geothermal gradient by penetrating an ordinary deep-sea heat flow probe, a heat flow piston corer (HFPC, cf. 3.4.2), or a Stand-Alone Heat Flow meter (SAHF, cf. 3.4.3) into seafloor sediments.

[Specification of tools]

The deep-sea heat flow probe has a 3.0 m or 4.5 m-long lance, along which seven thermistor temperature sensors are mounted in an outrigger fashion (Ewing type; Fig. 3.4-1). Three of the sensors contain heating wires for measurements of in-situ thermal conductivity using calibrated heat pulses. The total weight of the probe is about 800 kg and the lance is strong enough to allow multi penetrations at each station. Temperature of the sensors and two components of the instrument tilt are measured every 30 sec. The data are recorded in the data logger (Kaiyo Denshi Co., DHF-650) and sent to the surface with acoustic pulses so that we can monitor the status of the probe on the ship.

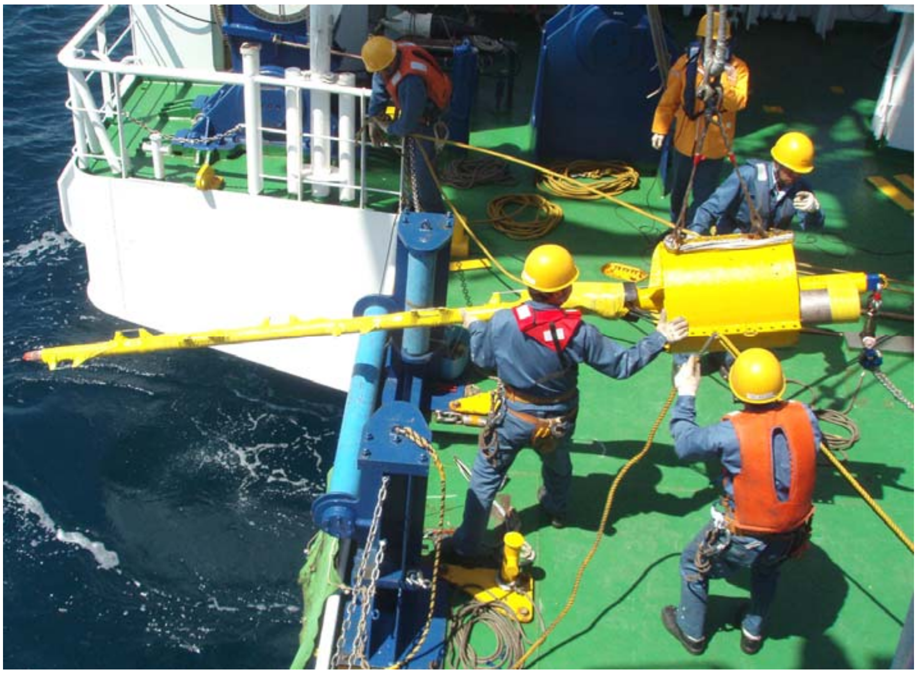

Figure 3.4-1. Deep-sea heat flow probe with Ewing type temperature sensors.

At some stations, we attached compact temperature recorders (Miniaturized Temperature Data Logger, ANTARES Datensysteme GmbH; Fig. 3.4-2) along the lance in stead of temperature sensors connected to the data logger.

Figure 3.4-2. ANTARES Miniaturized Temperature Data Logger (MTL).

Specifications of the data logger for the heat flow probe and the ANTARES Miniaturized Temperature Data Logger (MTL) are summarized below:

Heat Flow Data Logger DHF-650 (Kaiyo Denshi Co.)

Pressure case: titanium alloy

Case length: 725 mm

Maximum diameter: 145 mm

Pressure rating: 7000 m water depth

Number of temperature channels: 9

Temperature resolution: 1mK

Tilt: two-axis, 0 to ±45°

Data-cycle interval: 30 sec

Pinger frequency: 15.0 kHz (or 12.0 kHz)

Miniaturized Temperature Data Logger (ANTARES Datensysteme GmbH)

Pressure case: stainless steel

Case length: 160 mm

Diameter: 15 mm

Pressure rating: 6000 m water depth

Number of temperature channel: 1

Temperature resolution: 1.2 mK at 20°C, 0.75 mK at 1°C

Sample rate: variable from 1 sec to 255 min.

[Operations]

A 15 m long nylon rope was put between the heat flow probe and the winch wire rope in order not to kink the wire rope during probe penetrations. An acoustic transponder was attached 40 m above the probe for precise determination of the position of the probe and the distance from the seafloor (Fig. 3.4-3).

Multi-penetration heat-flow measurement operations were conducted following the procedures described below.

1. Measure water temperature about 50 m above the sea floor for calibration of temperature sensors.
2. Lower the probe at a speed of about 1 m/sec until it penetrates into the sediment.
3. Measure temperatures in the sediment for about 20 min. Monitor the wire tension and pay out the wire when necessary to keep the probe stable.
4. Pull out the probe and move to the next station.

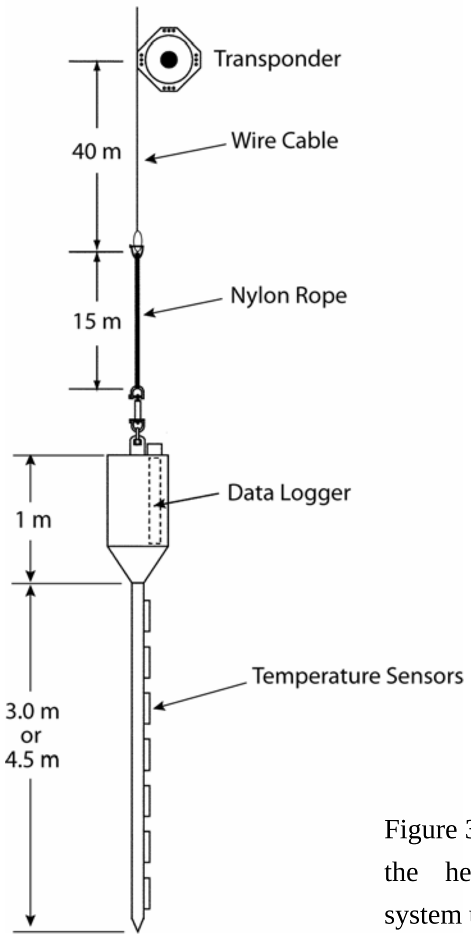

Figure 3.4-3. Configuration of the heat flow measurement system using a deep-sea probe.

3.4.2. Heat flow piston coring system

[Specification of tools]

During this cruise, sediment core samples were taken with the heat flow piston coring system (HFPC) (Fig. 3.4-4). This coring system was used for combined operation of measuring heat flow and recovering sediments. The general outline of the system is shown in Fig.3.4-5.

A stainless steel barrel was attached to a piston core head of 800 kg weight. The core head has a space for mounting the heat flow data logger to record the temperatures of thermistor sensors mounted along the barrel. On this cruise, six ANTARES MTLs (cf. 3.4.1) were mounted helically on the outside of barrel, between the base of the weight stand and the core catcher bit. A transponder was also mounted on the winch wire to obtain the water depth and position of this equipment. The stainless steel barrel with this system is 4 m in length and liner is used for recovering sediments. The balance and pilot corer are the same as ones for ordinary piston core systems. 24mm nylon rope was placed between the balance and winch wire for additional wire out and/or increased tension after hitting sea bottom. Because the system must be kept in the sediment for 15 to 20 minutes to obtain stable temperature, additional wire out is necessary for avoiding pulling the barrel out of the sea floor by either heaving or drifting of the ship during the measurement.

Figure.4-4. HFPC with compact temperature data loggers (MTLs).

[Operations]

<u>Preparation for the piston coring</u>

After barrels are attached to the head (weight stand), the main wire is connected, through the barrel, to the piston at the bottom of the barrel. The core catcher and bit are then attached. The balance is connected to the end of the main wire. The entire assemblage is carried under the A flame using a cart and is lifted over the edge of the deck by the winch, A flame and capstan winches, the pilot core and it’s wire are then connected to the balance. During the launch into the sea we have to add a large amount of water into the barrel from the top to prevent the piston moving due to water pressure from below. The system is then lowered through the water to the sea floor.

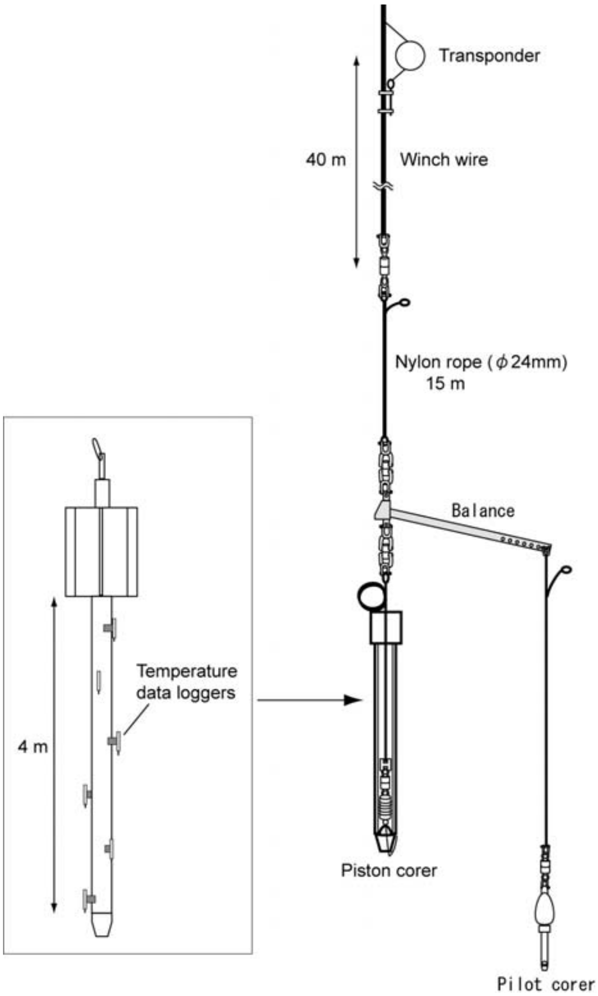

Figure 3.4-5. Configuration of the heat flow piston coring (HFPC) system.

<u>Hit the bottom and off the bottom</u>

The piston core system starts lowering at a winch speed of 20 m/min, which is gradually increasing to a maximum 60 m/min. The piston core is stopped at a depth about 60 m above the sea floor for 10 minutes to reduce any pendulum motion and to calibrate the temperature sensors on the outside of barrel.

After 10 minutes, the wire is lowered at a speed of about 20m/min., at the same time carefully watching the pen recorder of the strain gauge tension meter. When the piston core hit the bottom the tension will abruptly decrease by the amount of the piston core weight. Therefore, it is easy to detect the bottom hit.

After the recognition of hit the bottom, add 5m to wire out, stopped and keep the position for 20 minutes. And then, rewinding of the wire is started at a dead slow speed (～20 m/min.), until the tension gauge indicate that the core has lifted off the bottom. The tension meter shows a small increase in tension when the core is being pulled out of the sea floor and then a steady value. After we can recognize absolutely that the piston core is above the sea floor, the winch to keep speed is increased to 60m/min., and then gradually to maximum speed.

3.4.3. Stand-Alone Heat Flow meter (SAHF)

[Instrument]

Stand-Alone Heat Flow meter (SAHF) is designed to measure sub-seafloor temperature gradient with manned submersibles or ROVs (Fig. 3.4-6). SAHF runs "off-line" so that it gives operators time to conduct other operations during the measurement. Note that SAHF can also be used for long-term monitoring of sub-bottom temperature.

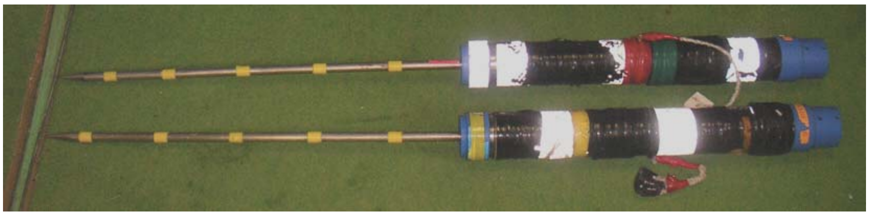

Figure 3.4-6: SAHF6 (top) and SAHF7 (bottom).

The pressure case contains an electric circuit and a battery, and the probe includes five thermistors with an 11 cm interval. The following table gives a brief description of SAHF6 and SAHF7, which we deployed in the present cruise.

Material	Alloy of titanium
Weight	4.0 kg in the air, 2.6 kg in seawater
Length of pressure case	525 mm
Diameter of pressure case	58 mm
Length of probe	600 mm
Diameter of probe	13.8 mm (filled with silicon oil inside)
Number of thermistors	5
Intervals of thermistors	110 mm
Accuracy	0.01 K
Resolution	0.001 K
External Interface	RS-232C (9600BAUD, 8 BIT, Non-Parity, 2 STOP BIT)

[Operation]

When KAIKO 7000II descends or ascends, SAHF is kept in its sample basket. After KAIKO lands on seafloor, SAHF is held by the manipulator.

For each measurement, SAHF first records the reference seawater temperature at rest for 5 minutes, and then is pushed vertically into the sediment. If penetration of at least three thermistors is not attained, penetration is attempted again. Measurement of sub-seafloor temperature gradient takes 15-20 minutes in order to obtain reliable data. Note that when multiple measurements are conducted at the same place, measurement of reference seawater temperature can be skipped.

3.4.4. Long-term temperature monitoring systems

For heat flow measurement at stations with water depths less than 2000 m, we used two types of long-term temperature monitoring systems.

[Pop-up heat flow instrument (PHF)]

We developed pop-up type heat flow probes that can record temperatures in the surface sediment for more than one year. Long-term sediment temperature records up to about 400 days have been obtained with these instruments at ten stations in shallow sea areas off Shikoku and off the Ki-i Peninsula. At eight stations where temperature records longer than 220 days were obtained, we could determine the temperature gradient and heat flow by removing the effect of the bottom water temperature variation from the raw temperature data (Hamamoto et al., 2005).

On KR08-10 cruise, we conducted calibration tests of two pop-up heat flow instruments (termed PHFs below; Fig. 3.4-7) and deployed them. The basic configuration and specification of the two instruments are essentially the same. Main components of PHF are a recording unit, a temperature probe and a weight (Fig. 3.4-8). The temperature probe is 2 m long and has six or seven temperature sensors set at even intervals. The recording unit records the measurement date and time, temperatures, and two-axis instrument tilts. The temperature resolution is 1 mK. A small water temperature recorder (NWT-DN, Nichiyu Giken Kogyo Co.) is attached to the main frame for monitoring the bottom water temperature. After recording the sediment temperatures, the PHF releases the weight and temperature probe responding to an acoustic command, and the recording unit pops up and can be recovered with a surface ship.

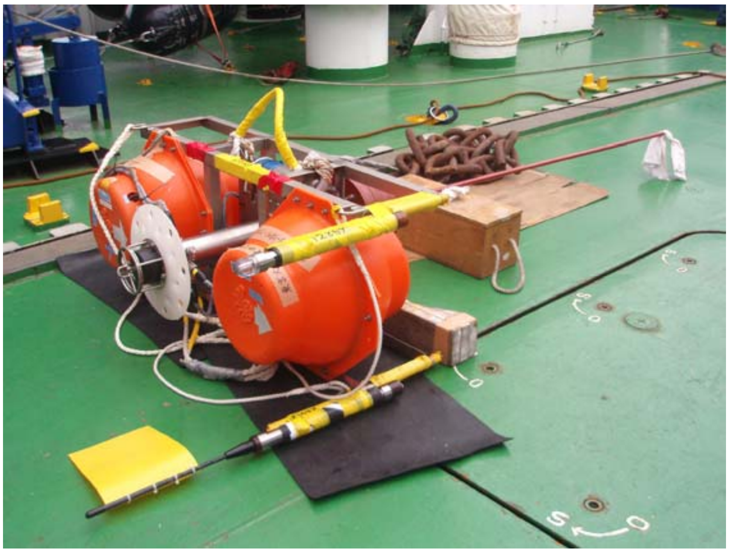

Figure 3.4-7. Pop-up heat flow instrument (PHF) lying on the deck.

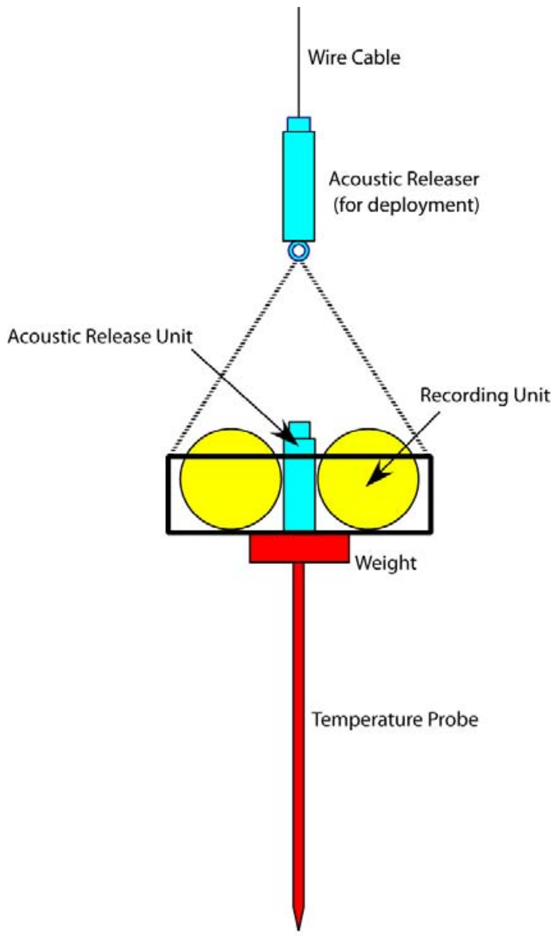

Figure 3.4-8. Schematic configuration of PHF.

Specifications of the water temperature recorder (NWT-DN) are summarized below.

Pressure case	titanium alloy
Case length	212 mm
Diameter	41 mm
Pressure rating	6000 m water depth
Number of temperature channel	1
Temperature resolution	1 mK
Sample rate	variable from 2 sec to 1 day

For accurate determination of the temperature gradient, it is necessary to calibrate the temperature sensors by measuring the deep water temperature, which is spatially quite uniform. We usually lower PHF down to 1000 to 2000 m depth and measure the water temperature for about 30 min. This temperature record is used for analyses of long-term sediment temperature data.

When we deploy PHF, an additional acoustic releaser is set between the PHF and the winch wire rope (Fig. 3.4-8). The PHF is lowered to about 30 m above the sea floor, monitoring the depth of the instrument using a transponder attached to the winch cable. Then an acoustic command is sent to activate the releaser and the PHF falls freely to penetrate into the sediment.

[Pop-up water temperature measurement system (PWT)]

Heat flow data in shallow sea areas can be obtained through long-term temperature monitoring with PHFs. It is not easy, however, to conduct measurements with PHFs at many stations, since the monitoring period needs to be quite long, about one year, and the instruments are relatively expensive. If we obtain bottom water temperature records at additional stations, we may be able to clarify the general pattern and features of bottom water temperature variations in the study area. Such information will be helpful in determination of appropriate length of the monitoring period for PHFs. Moreover, it is possible to determine heat flow by analyzing the temperature profile measured with ordinary deep-sea probes in combination with the preceding bottom water temperature records.

We have been using a pop-up water temperature measurement system (termed PWT below) in order to obtain long-term bottom water temperature records (Fig. 3.4-9). PWT consists of an acoustic releaser, weights, floats (glass spheres), and a small water temperature recorder (NWT-DN) (Fig. 3.4-10). For deployment, the whole system is released at the sea surface and it sinks freely down to the sea floor. The system is recovered by activating the acoustic releaser with a command sent from a surface ship.

On KR08-10 cruise, we recovered one PWT which was deployed in October, 2007 and deployed two PWTs.

Figure. 3.4-9. Pop-up water temperature measurement system (PWT).

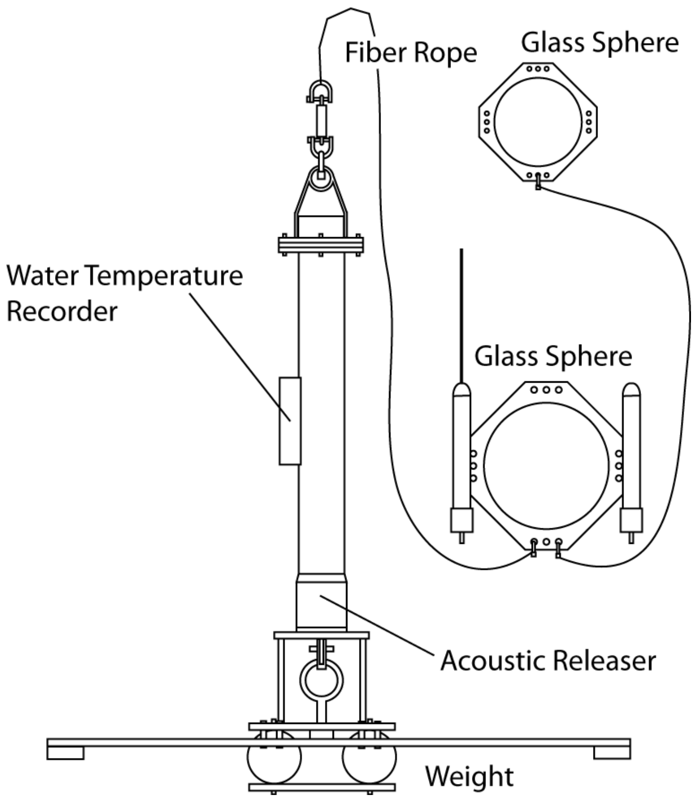

Figure 3.4-10. Schematic drawing of PWT.

3.4.5. Physical properties of core samples

[Thermal conductivity]

We need to know thermal conductivity of surface sediments in order to obtain heat flow values. Thermal conductivity of piston core samples was measured using two different types of line-source commercial devices. One is KD2 Pro (Decagon Devices) with a full-space type needle probe (von Herzen and Maxwell, 1959). The probe was inserted into whole-round core samples. The other is QTM-500 (Kyoto Electronics Manufacturing Co.) with a half-space type box probe (Sass et al., 1984). Measurements with this instrument were made on split core samples.

[Magnetic susceptibility]

In order to know successive magnetic susceptibility throughout whole piston cores, we used Magnetic Susceptometer MS2 (Bartington Instruments) with a loop sensor. This measurement system was borrowed from Dr. Toshiya Kanamatsu (IFREE 1, JAMSTEC).

[Shear strength]

In order to understand shear strengths of core samples under the undrainage and unconsolidation (UU) conditions, we conducted vane shear test. The shear strength is measured using four-wing-bearing torque driver of 2 cm in height and 1 cm in width. The measurement has done as follows; 1) the whole wings of the torque driver were penetrated directly into the splitting surface of the working half after cube sampling, 2) the torque driver was rotated slowly, 3) record the torque force by 1 second interval. Each test was done for approximately 20 seconds. If the sediment samples were too hard to measure, the penetration depth of the wings was changed from 2 cm to 1 cm, and measured again for 20 seconds at new surface.

The shear strength is calculated by the shear friction working during rotation of the driver. According to the vane rotation length, it is calculated the one unit on the driver is 4.54 kPa as below calculation.

$$C = \frac{M_{t\,\max}}{\pi D^2 \left(\frac{H}{2} + \frac{D}{6} \right)}$$

where C is the shear strength (kg / cm^2), $M_{t\max}$ is the torque moment (kg cm), H is the wing height (cm), and D is the total wing width (cm).

3.4.6. Ocean-bottom electromagnetometer (OBEM)

[HF-OBEM]

We used a short-term or high-frequency OBEM (HF-OBEM) in this cruise. The HF-OBEM was developed by JAMSTEC in 2005, internally called as “JM100” type. The HF-OBEM consists of a 17-inches glass sphere, a 10-inches glass float, a magnetometer case, a transponder and four long arms (Figs. 3.4-11, 3.4-12).

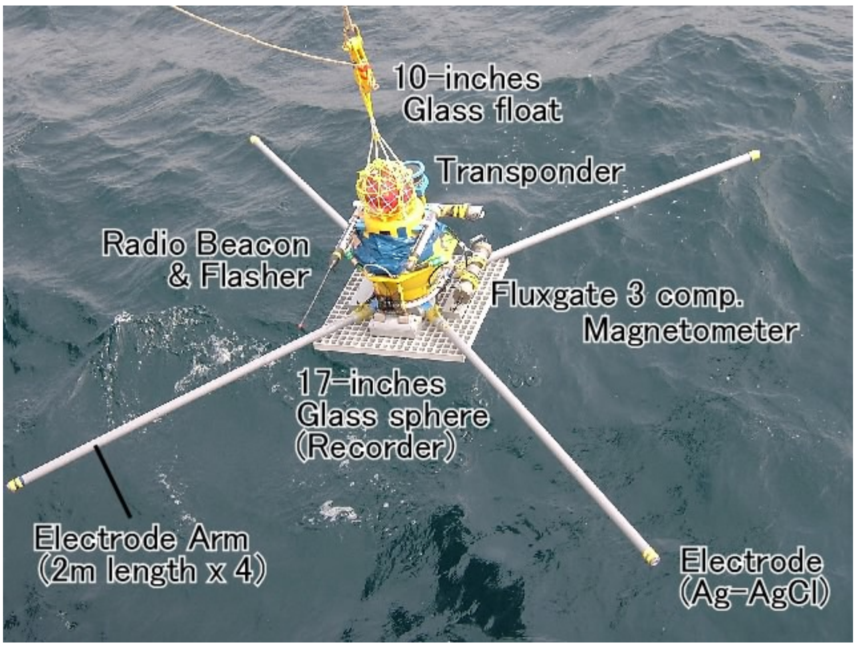

Figure 3.4-11. HF-OBEM (JM100 type).

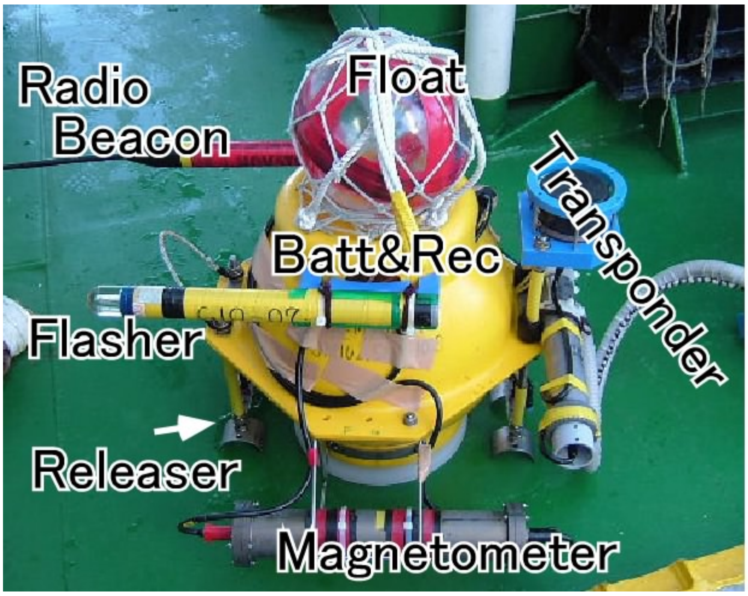

Figure 3.4-12. Central unit of HF-OBEM.

Major electrical circuits are packed into the 17-inches glass sphere. The main sensors of HF-OBEM are a magnetometer, a tilt meter, a voltmeter and a thermometer, all made by Tierra Technica, Japan. The magnetometer is a three-component Fluxgate type. It can record fluctuations of the vector geomagnetic field with 0.01 nT resolution. The sensor itself is not packed with the main circuit, but installed in another aluminum pressure case for reducing the magnetic noise from the circuit. The tilt meter with 0.26 mK resolution is also installed with the magnetic sensor. The voltmeter can record two horizontal components of electric field on the seafloor with about 0.3 μV resolution. The Ag-AgCl electrodes, made by Clover Tech., are set at the tip of arms (Fig. 3.4-13). The DC voltage differences between electrodes used in this cruise are summarized in Table. 3.4-1. The thermometers record temperature at the main circuit and the magnetic sensor. The lithium battery pack for these circuits is set in the same glass sphere. By using this battery pack, the HF-OBEM can record the EM field continuously for about a month, with the sampling rate of 8 Hz.

Table 3.4-1. DC voltage differences between Ag-AgCl electrodes

electrode	mV	electrode	mV
Site101N-GND	-0.17	Site102N-GND	0.29
Site101S-GND	-0.20	Site102S-GND	0.21
Site101E-GND	-0.15	Site102E-GND	0.24
Site101W-GND	-0.23	Site102W-GND	0.13
Site101COM-GND	-0.11	Site103N-GND	0.08
		Site103S-GND	0.10
		Site103E-GND	0.07
		Site103W-GND	0.11

Figure 3.4-13. Ag-AgCl electrodes. They are normally soaked in the salt water tank, and checked with measuring the voltage differences between electrodes.

The acoustic transponder, made by Kaiyo Denshi was used for recovering the OBEM with self pop-up. The transponder can reply to the signal from ship's SSBL system, so that the landing position of OBEM can be decided quickly. Also, the descending and ascending OBEM can be traced with the SSBL system. The transponder can receive an acoustic command for releasing the weight with lead. After receiving the command, the electric current from transponder corrodes and cuts the stainless plate between the grass sphere and the weight (Fig. 3.4-14), then the OBEM start to pop up with its own buoyancy.

Fig. 3.4-14. Releasing unit. A stainless plate (SUS), connecting the glass sphere and the weight, is cut after receiving an acoustic command.

The HF-OBEM can fold the electrode arm after launching from the seafloor. It is effective for increasing the ascending speed of OBEM and picking up the OBEM from the sea surface.

[LT-OBEM]

The long-term OBEMs (LT-OBEMs) are made by Tierra Technica, which can measure time variations of three components of magnetic field, horizontal electric field, the instrumental tilts, and temperature. The resolutions are 0.01 nT for flux-gate magnetometer, 0.305 μV for voltmeter, 0.00026 degrees for tiltmeter, and 0.01°C for thermometer. There are two types of instrumental design (Fig. 3.4-15). Type 1 LT-OBEM is equipped with three glass spheres on an aluminum frame, housing Benthos acoustic transponder, the electromagnetometer, and a Lithium battery pack for the electromagnetometer, respectively. Type 2 LT-OBEM is an improved version of type 1, which is equipped with two glass spheres on a titanium frame. An acoustic transponder and the battery pack are put together in one glass sphere. We have one type-1 LT-OBEM (TT4) and one type-2 LT-OBEM (TT1). On all the LT-OBEMs, a radio beacon, a flash light, and a catching buoy for easy recovery are mounted.

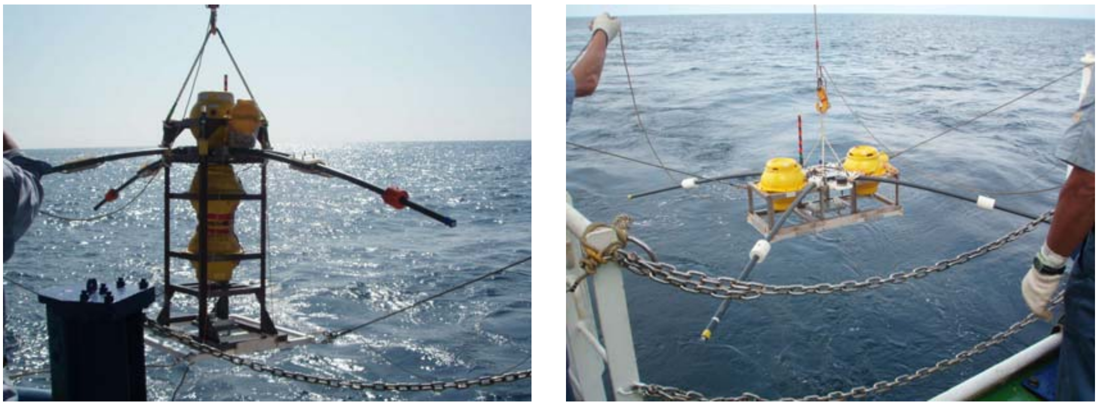

Figure 3.4-15. Type 1 LT-OBEM (left) and Type 2 LT-OBEM (right).

For electric field measurements, Ag-AgCl equilibrium electrodes made by Clover Tech. were utilized. The electrodes were monitored their self potentials in laboratory in advance of the seafloor observation and were selected pairs that the coherence is high enough, in order to reduce the noise due to the voltage drift of electrodes themselves. The monitored data were plotted in Figs. 3.4.-16 and 3.4-17.

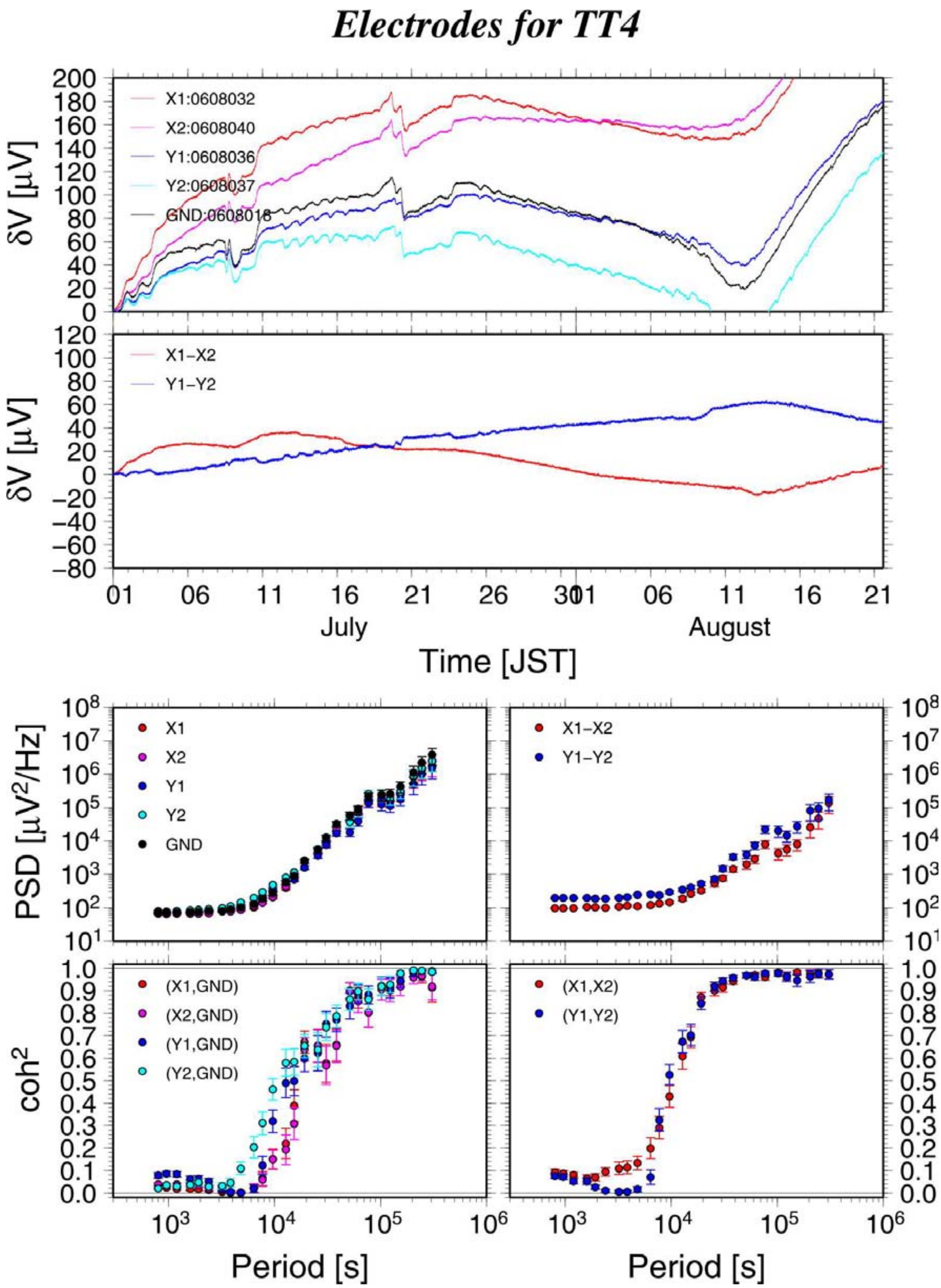

Figure 3.4-16. Electrodes selected for LT-OBEM TT4. From the top to the bottom, the time series of voltage differences to a common electrode and between pairs, power spectrum densities, and squared coherences are plotted, respectively.

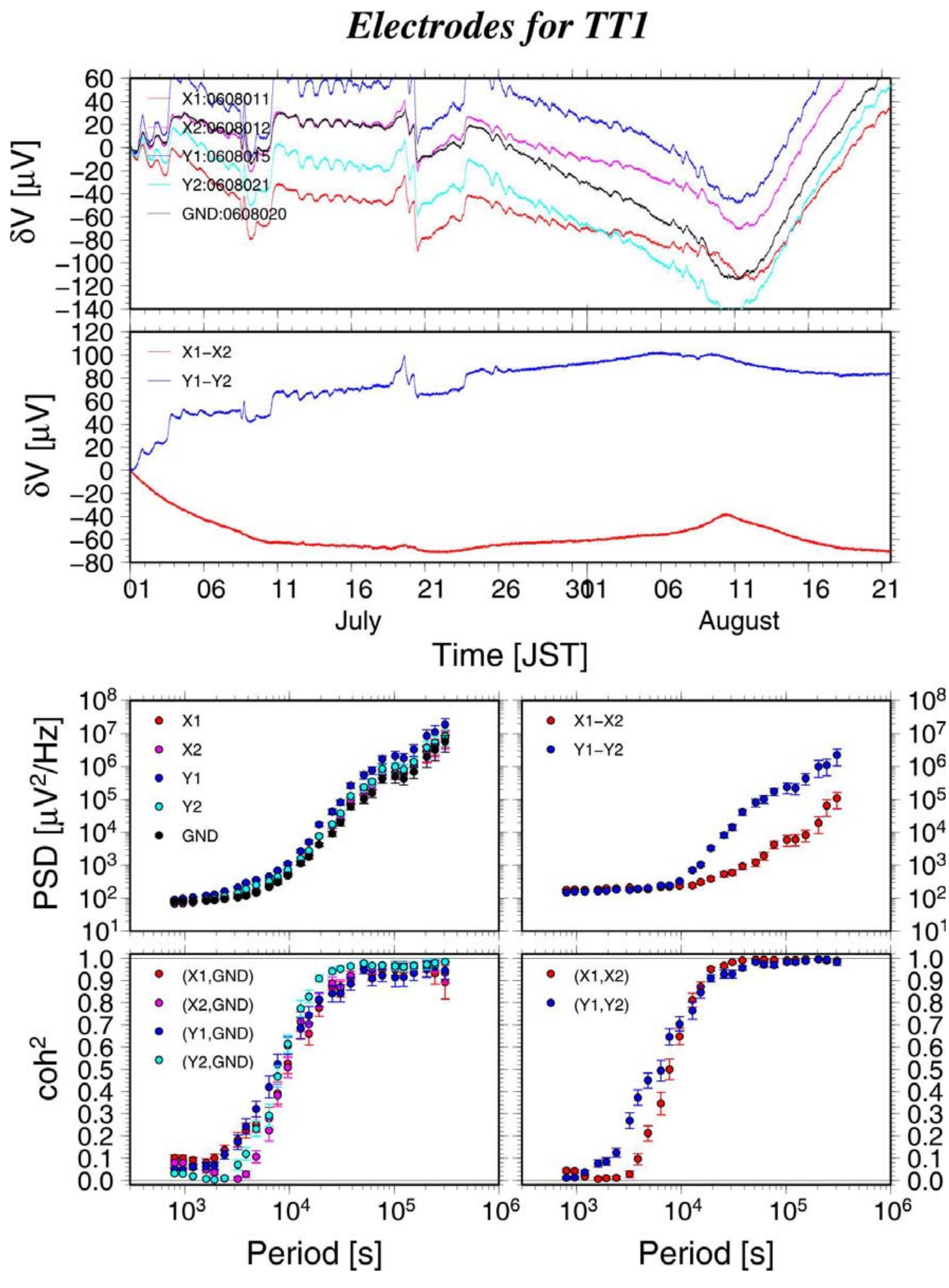

Figure 3.4-17. Electrodes selected for LT-OBEM TT1. The plotted contents are the same as Fig. 3.4-16.

3.4.7. KAIKO CSEM system

On this cruise, we tested a newly developed controlled-source electromagnetic (CSEM) system operated by the ROV KAIKO 7000II. The schematic explanation of the system is shown in Fig. 3.4-18. The detail of the system is explained in the following photos (Fig. 3.4-19). At the first dive (Dive#428), we tested the system in the middle of deep water (at about 1000m water depth) where the seafloor is located 500m below the ROV KAIKO 7000II. At the second dive, we went to the seafloor with depth of about 5200 m, extended the CSEM cable, and shot the artificial electric current through the cable.

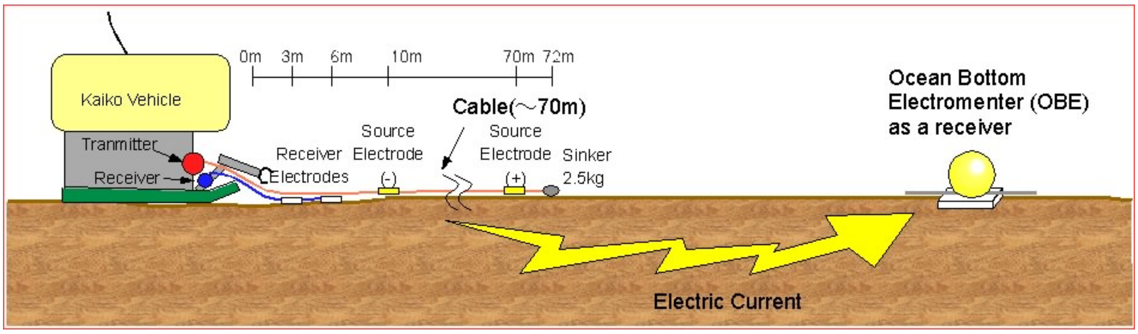

Figure 3.4-18. Concept of the KAIKO CSEM experiment.

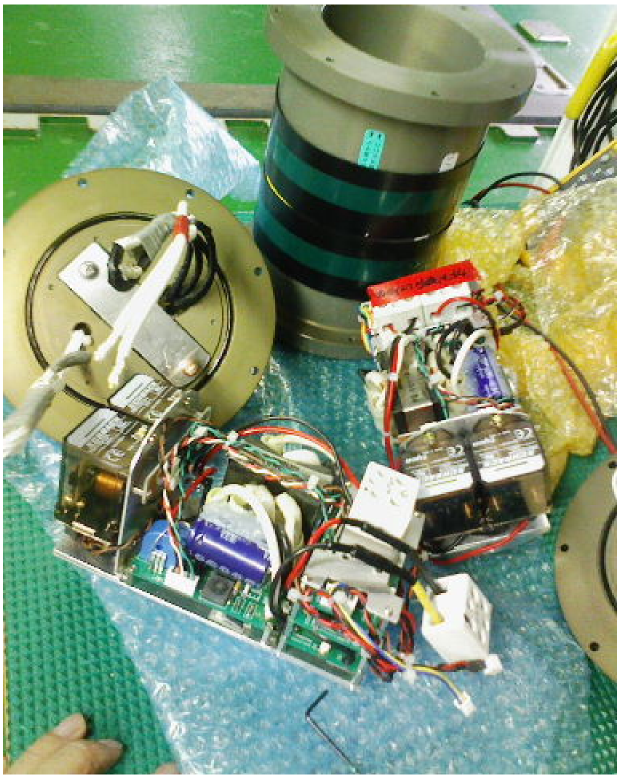

Figure 3.4-19. Details of the KAIKO CSEM. (a) Transmitter circuits.

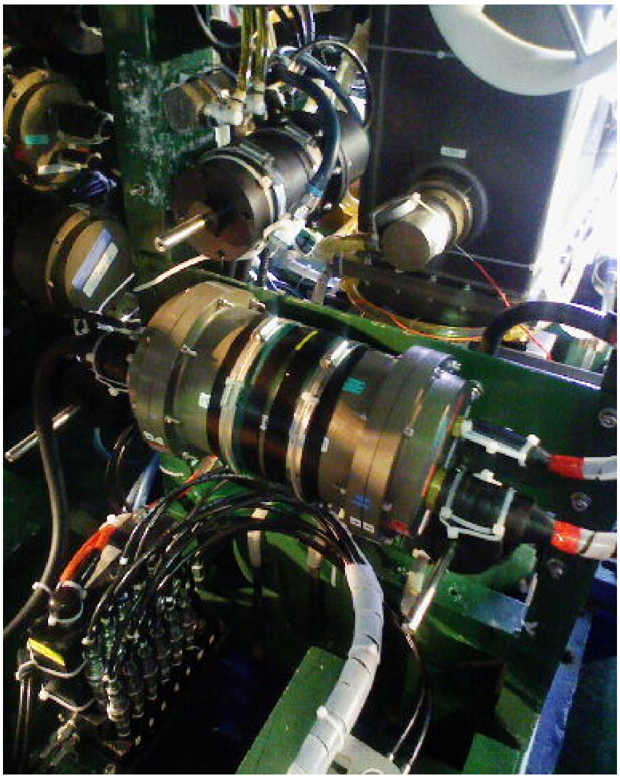

Figure 3.4-19.　(b) Transmitter with pressure case.

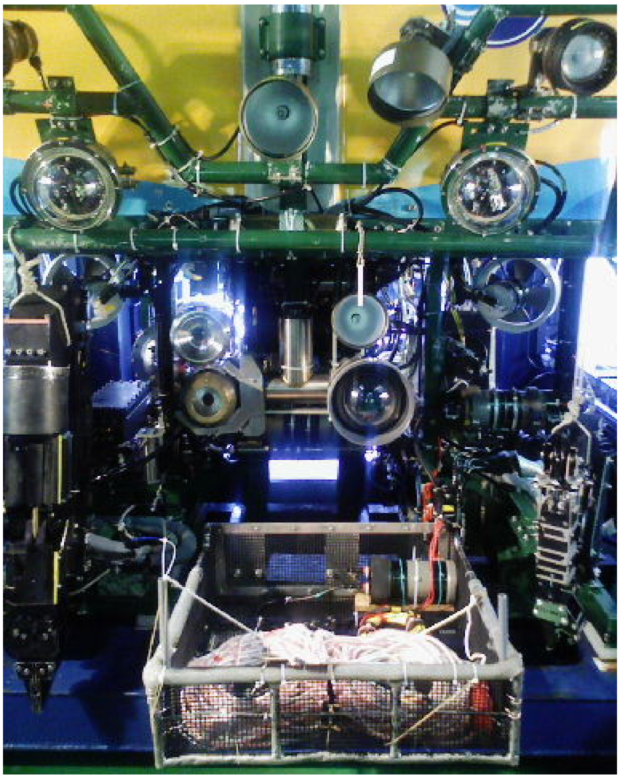

(c) Transmitter is attached at the base of left arm.

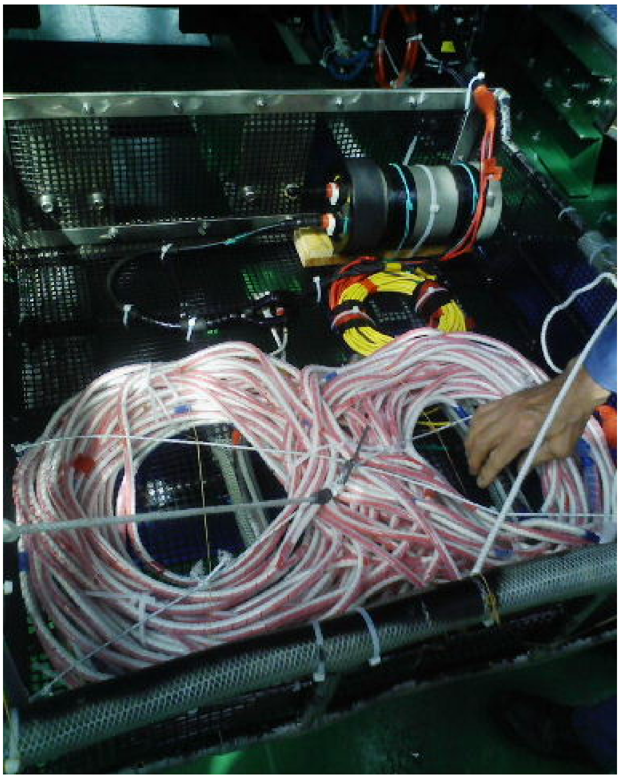

Figure 3.4-19.　(d) Cable for transmitting electric current.

Figure 3.4-19. (e) Receiver electrode (upper) and source electrode (lower).

Figure 3.4-19.　(f) Sinker at the end of cable

3.5. Preliminary Results

3.5.1. Heat flow measurement

We carried out heat flow measurements at 16 sites with the deep-sea heat flow probe, at 6 sites with the HFPC and at 2 sites with the SAHF (Table 3.5-1; Fig. 3.2-2). At all the sites with the deep-sea heat flow probe, multiple penetrations were attempted for examining local variability of heat flow. The probe did not penetrate into sediment at some stations ("fell" in Table 3.5-1). At SAHF stations #429SF1 and #429SF2, no data were obtained due to a problem with temperature sensors. The coordinates of the stations listed in Table 3.5-1are the positions of the transponder attached just above the probe or HFPC or KAIKO 7000II determined with the SSBL system of the ship, while the water depth in the table is the depth right below the ship and may be slightly different from the depth at the station.

Most of the stations are located on the seaward side of the Japan Trench along the 40°15'N survey line, extending from the upper part of the trench slope to the top of the outer rise (between 144°43'E and 146°27'E). Deep penetration of the probe and the corer could not be attained around 145°15'E to 145°30'E (HF03, HF05, and HFPC02). It is probably due to volcanic ash layers at shallow depths, which were recovered at HFPC02 (cf. 3.5.3).

Sites HF06, HF07, HF12, HF13, HF14, HF16, HFPC04, HFPC05, and HFPC06 are located on the landward side of the trench, either along the 40°15'N survey line or along another line on which multichannel seismic reflection survey was made around 39°N (Tsuru et al., 2000). Temperature profiles measured at sites with water depths shallower than 2000 m (HF07, HF12, HFPC04, and HFPC06) are clearly disturbed by temporal variation of the bottom water temperature. They need to be analyzed with long-term records of bottom water and sediment temperatures. HF12 is in the vicinity of the stations where a PWT was recovered and a PHF was deployed on this cruise (PWT02 and PHF02). HF07, HFPC4, and HFPC06 correspond to PHF01, PWT01, and PWT03 respectively, where we deployed a PHF and PWTs on this cruise. At sites with water depths of about 3000 m (HF06, HF13, and HFPC05), the effect of the bottom water temperature variation appears to be less but may not be negligible. We should attempt to evaluate the effect around this water depth through long-term temperature monitoring.

Thermal conductivity measurement with the pulse heating method was attempted at most stations where the deep-sea probe was used. We will analyze the temperature data at these stations to determine in situ thermal conductivity values. The obtained values should be compared with those measured on piston core samples (cf. 3.5.3) to estimate average thermal conductivity of surface sediment at each site, which is used for calculation of the heat flow.

Table 3.5-1. Results of heat flow measurements

Date	Station	Latitude (N)	Longitude (E)	Depth (m)	N
Deep-sea heat flow probe					
Aug. 20	HF01A	40°15.08'	145°40.47'	5230	2
	B	40°15.02'	145°40.45'	5225	2
	C	40°14.99'	145°40.18'	5230	3
	D	40°14.99'	145°39.88'	5240	3
Aug. 21	HF02A	40°15.04'	146°26.51'	5225	2
	B	40°15.04'	146°26.27'	5220	2
Aug. 22	HF03A	40°15.03'	145°24.97'	5400	2
	B	40°15.08'	145°24.74'	5395	fell
	C	40°15.05'	145°24.76'	5400	fell
	D	40°15.04'	145°24.77'	5395	fell
	E	40°15.04'	145°24.74'	5395	fell
	HF04A	40°14.95'	145°09.99'	5655	5
	B	40°14.94'	145°10.19'	5630	5
Aug. 23	HF05A	40°15.00'	145°13.98'	5560	fell
	B	40°15.00'	145°13.98'	5560	fell
	C	40°15.00'	145°14.00'	5560	2
	D	40°14.98'	145°14.17'	5550	fell
	E	40°15.00'	145°14.18'	5550	fell
	F	40°15.23'	145°14.16'	5550	3
	G	40°15.01'	145°14.27'	5555	2
Aug. 24	HF06A	39°09.02'	143°30.95'	3075	5
	B	39°09.02'	143°30.95'	3080	5
	C	39°09.26'	143°30.95'	3080	5
	E	39°09.33'	143°30.94'	3095	5
Aug. 26	HF07A	39°13.99'	142°58.48'	1770	7
	B	39°13.99'	142°58.49'	1775	7
Aug. 27	HF08A	40°15.09'	144°43.59'	6280	3
	B	40°15.06'	144°43.80'	6245	3
	C	40°15.03'	144°43.87'	6265	3
Aug. 28	HF09A	40°15.00'	145°57.00'	5160	4
	B	40°14.98'	145°57.29'	5155	4
	C	40°14.97'	145°57.33'	5160	4
	D	40°14.97'	145°57.34'	5155	4

Date	Station	Latitude (N)	Longitude (E)	Depth (m)	N
Aug. 28	HF10A	40°15.08'	145°40.55'	5220	7
	B	40°15.07'	145°40.54'	5225	7
	C	40°14.99'	145°40.77'	5225	7
	D	40°14.98'	145°40.80'	5220	5
Aug. 29	HF11A	40°15.01'	145°01.99'	5740	4
	B	40°15.07'	145°02.19'	5740	4
	C	40°15.08'	145°02.46'	5730	4
	D	40°15.15'	145°02.89'	5745	fell
	E	40°15.26'	145°03.79'	5860	4
	F	40°15.16'	145°04.16'	5825	5
	G	40°15.11'	145°04.41'	5810	fell
Aug. 30	HF12A	40°15.05'	142°58.95'	1420	5
	B	40°15.06'	142°58.93'	1420	5
	C	40°14.99'	142°58.63'	1420	5
	D	40°14.96'	142°58.42'	1420	5
Aug. 31	HF13A	40°15.02'	143°43.02'	2900	5
	B	40°15.02'	143°43.04'	2905	5
	C	40°14.99'	143°42.67'	2880	6
	D	40°14.99'	143°42.64'	2880	6
	E	40°14.99'	143°42.35'	2875	6
	G	40°14.98'	143°42.34'	2865	6
Sep. 6	HF14A	40°15.02'	144°04.98'	4740	7
	B	40°15.03'	144°04.97'	4745	7
	C	40°15.02'	144°04.98'	4740	7
	D	40°14.92'	144°04.84'	4745	7
	E	40°14.90'	144°04.83'	4745	7
Sep. 7	HF15A	40°15.02'	145°39.84'	5230	6
	B	40°15.01'	145°40.27'	5220	6
	C	40°15.02'	145°40.56'	5215	5
	D	40°15.00'	145°41.26'	5205	6
	E	40°14.99'	145°41.61'	5210	4
Sep. 9	HF16A	39°07.98'	143°56.37'	5385	6
	B	39°08.00'	143°56.37'	5395	6
HFPC					
Aug. 21	HFPC01	40°15.04'	146°13.99'	5180	5

Date	Station	Latitude (N)	Longitude (E)	Depth (m)	N
Aug. 23	HFPC02	40°15.01'	145°29.96'	5315	3
Aug. 27	HFPC03	40°15.03'	144°57.99'	5815	4
Aug. 30	HFPC04	40°15.02'	143°03.50'	1425	6
Sep. 6	HFPC05	40°14.94'	143°42.29'	2890	6
Sep. 8	HFPC06	39°14.99'	142°51.07'	1700	6
SAHF					
Sep. 3	#429SF1	40°14.71'	145°24.92'	5425	no data
	#429SF2	40°14.80'	145°24.91'	5425	no data
Sep. 4	#430SF1	40°14.90'	145°41.22'	5220	5
	#430SF2	40°14.90'	145°41.22'	5220	5
	#430SF3	40°14.82'	145°41.17'	5220	5
	#430SF4	40°14.82'	145°41.17'	5220	5

N: number of temperature sensors used to obtain temperature profile in sediment.

3.5.2. Long-term temperature monitoring

We deployed pop-up heat flow instruments (PHFs; cf. 3.4.4) at two stations with water depths shallower than 2000 m for obtaining long-term records of temperature profiles in surface sediment (PHF01 and PHF02; Table 3.5-2; Figs. 3.2-2 and 3.5-1). The instruments have six or seven temperature sensors in 2-m long probes and the sampling interval was set as 20 min. They will be recovered after monitoring for about one year and the obtained sediment temperature records will be analyzed to determine the heat flow.

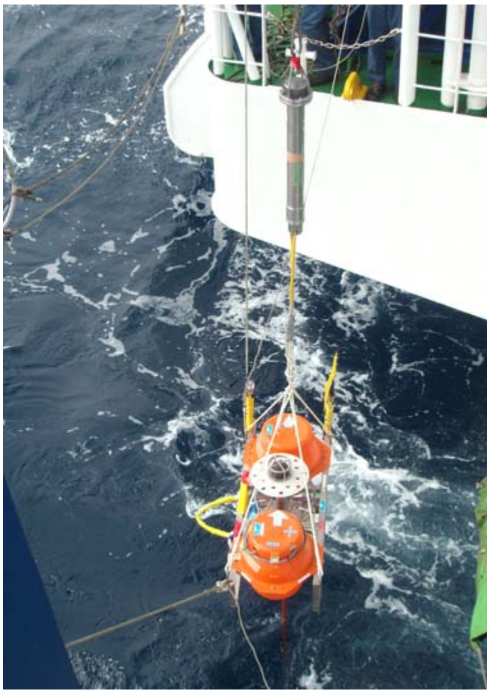

Figure 3.5-1. Deployment of a pop-up heat flow instrument (PHF).

Table 3.5-2. Deployment of PHF

Station	Date of deployment	Coordinates	Water depth (m)
PHF01	Aug. 26, 2008	39°14.0'N, 142°58.5'E	1830
PHF02	Aug. 30, 2008	40°15.1'N, 142°59.0'E	1420

We successfully recovered a pop-up water temperature measurement system (PWT; Table 3.5-3; Fig. 3.2-2), which was deployed on KH-07-3 cruise of R/V Hakuho-maru in October, 2007. This site (PWT02) is essentially the same as the station PHF02. The obtained bottom water temperature record is shown in Fig. 3.5-2. It shows large temperature variation, over 0.6 K, demonstrating that temperature in surface sediment has been significantly disturbed by bottom water temperature variation in areas with relatively shallow water depths (e.g., shallower than 2000 m).

Table 3.5-3. Monitoring of the bottom water temperature

Station	Deployment	Recovery	Coordinates	Water depth (m)
PWT01	Aug. 26, 2008		39°14.9'N, 142°51.2'E	1710
PWT02	Oct. 29, 2007	Aug. 31, 2008	40°15.0'N, 142°59.3'E	1420
PWT03	Aug. 31, 2008		40°15.1'N, 143°03.5'E	1420

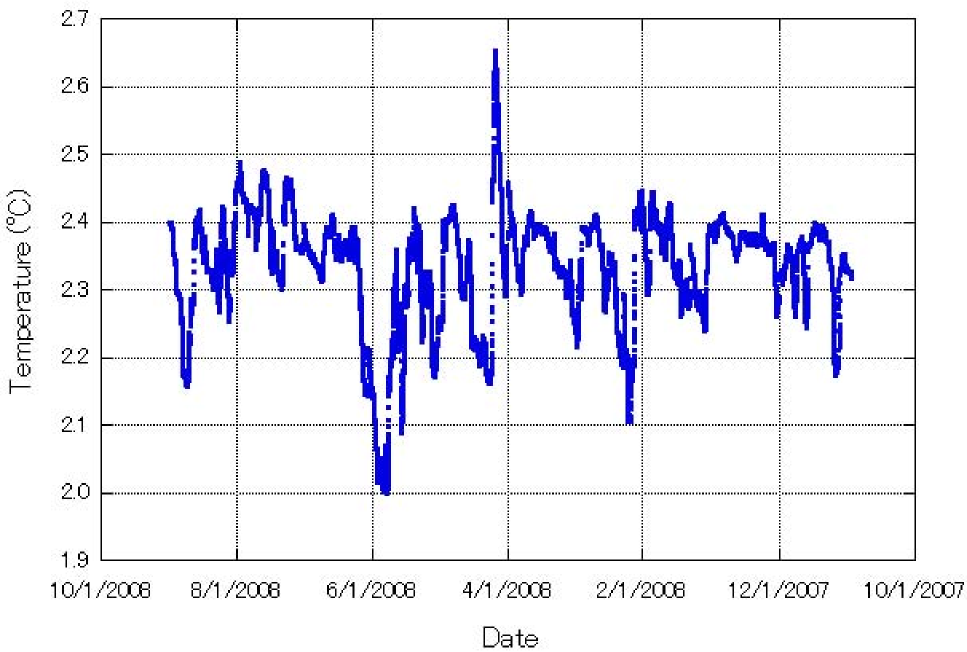

Figure 3.5-2. Bottom water temperature records at PWT-1 (top) and PWT-3 (bottom).

We deployed PWTs at two stations (PWT01 and PWT03; Table 3.5-3; Figs. 3.2-2 and 3.5-3). They will be recovered about one year after deployment.

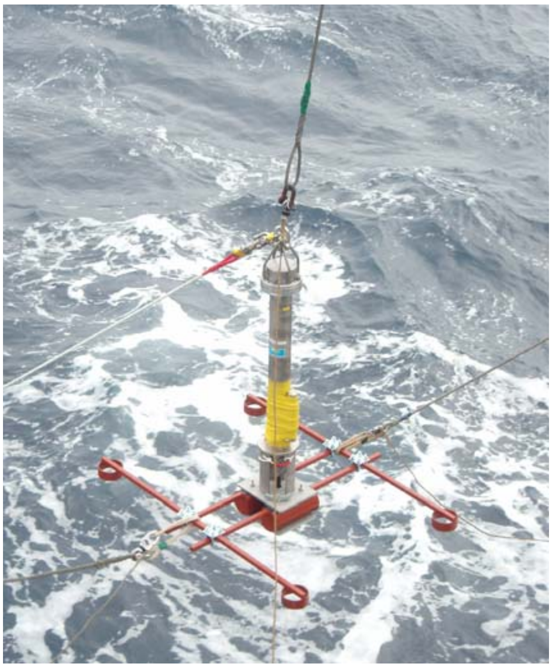

Figure 3.5-3. Deployment of a pop-up water temperature measurement system (PWT).

3.5.3. Piston core samples

Six piston core samples were collected off Hachinohe and off Miyako, northeast Japan (Table 3.5-1; Fig. 3.2-2) using 4-m-piston-corer system (cf. 3.4.2). The piston corer system has a pilot corer, so that two cores of a piston core sample and a pilot core sample were collected from one coring site. Six temperature data loggers (ANTARES MTLs, cf. 3.4.1) for heat flow measurement were attached to the core barrel of the piston corer to be a heat-flow piston corer (HFPC). Sample names of piston cores and pilot cores are HFPC (01, 02, 03, 04, 05, 06) and HFPL (01, 02, 03, 04, 05, 06), respectively.

The piston core samples were processed as follows (cf. 3.4.5);

1) Cut the whole core by 1 m section.
2) Measure magnetic susceptibility by 2 cm intervals using Bartington MS2 system with a loop sensor.
3) Measure thermal conductivity using a needle probe.
4) Split the whole core into working half and archive half.
5) Measure thermal conductivity of the archive half using a QTM instrument.
6) Describe the working half by naked eyes and smear slides.
7) Take photographs of the working half.
8) Measure shear strength of the core samples of the working half using vane shear tester.

9) Take samples successively from the working half using 7-cc-plastic-cubes.

Finally all the core samples were packed into D-tubes, then transported to the Kochi Institute for Core Sample Research, JAMSTEC.

The recovered six core samples (Fig. 3.5-4) are described in detail below. In addition, we recovered a push core sample from a flat floor near the Hokkaido Rise (outer rise of the Japan Trench) using ROV KAIKO 7000II (7K#430 C-1). This core is also described below.

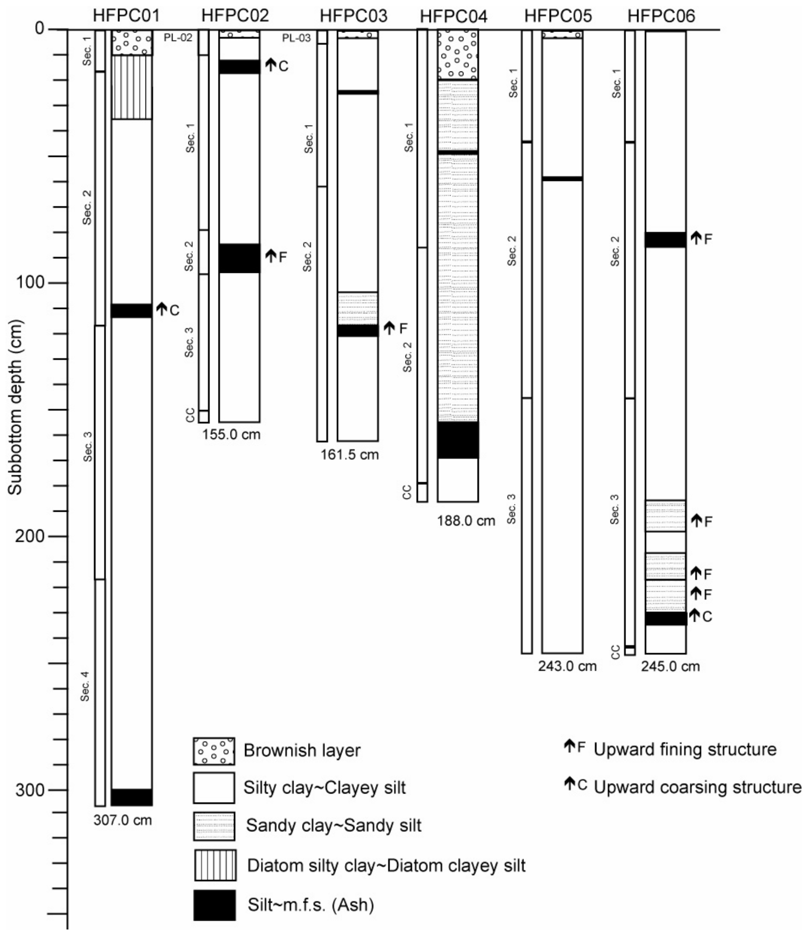

Figure 3.5-4. Lithological units of the piston cores.

[HFPC01 and HFPL01]

To measure the heat flow along the previous multi-channel survey line of 40°15’, HFPC01 was conducted on a flat surface in the Hokkaido Rise at 40°15.04’N and 146°13.99’E. The water depth was 5180 m. At this coring site, parallel continuous layer structures were seen in a subbottom profile image.

The piston and pilot cores are 307 cm and 77 cm long, respectively (Fig. 3.5-5). The core sediment is predominantly olive black (10Y3/2) clayey silt to silty clay with diatoms, which is composed of mostly siliciclastic grains, diatoms, volcanic glass and clay particles. The clayey silt has pyritized burrows filled with grayish mud in places. The silty clay is interbedded with dark greenish gray (10GY3/1) faint laminae in places. Grayish volcanic ash layers are seen at 112 - 116 cm-below-sea-floor (hereafter cm-bsf) and 300 - 307 cm-bsf. Just below the bottom of the core, two lapilli-sized pumices are in the core catcher (but most of the material in the core catcher were lost during the operation).

The magnetic susceptibility is fluctuated between 1 and 2 x 10^{-3} SI. In the bottom of Section 2, the magnetic susceptibility increase drastically 8 x 10^{-3} SI. This high magnetic susceptibility corresponds to the volcanic ash layer of 112 - 116 cm-bsf. Shear strength increases progressively from about 0 to about 15 kPa with increasing depth, because of burial consolidation of the sediments.

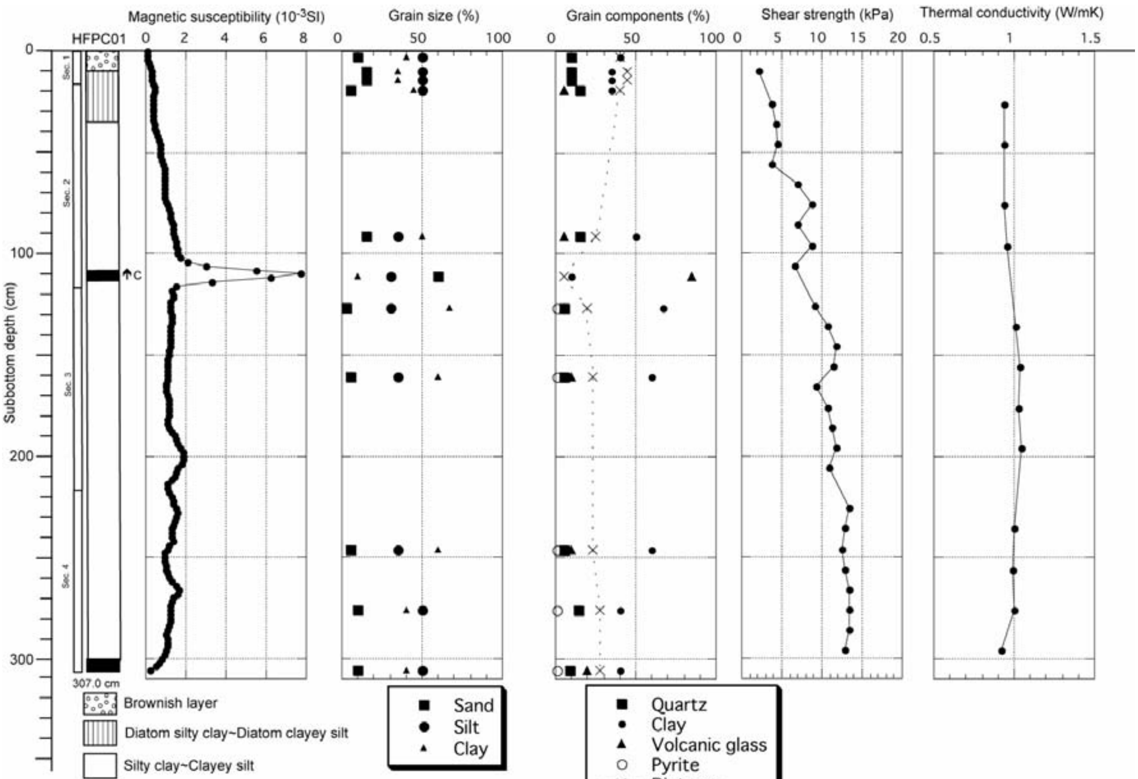

Figure 3.5-5. HFPC01.

[HFPC02 and HFPL02]

To measure the heat flow along the previous multi-channel survey line of 40°15’, HFPC02 was conducted on a seaward gentle slope at 40°15.01’N and 145°29.96’E. The water depth was 5315 m. At this coring site, parallel continuous layer structures were seen in a subbottom profile image.

The piston and pilot cores were recovered 270 and 34.5 cm long, respectively (Fig. 3.5-6).

But the pilot core penetrated probably twice into the seabed, because a surface oxidized layer can be seen at two horizons of 0 - 5.5 and 12 - 15.5 cm. Therefore original length of the pilot core by the first penetration is probably 12 cm long, and that of the second penetration is about 19 cm long or more.

Flow-in sediments can be seen between 85 and 212 cm from the top of the core. The surface oxidized layer of about 12 cm long blew out and it was lost. Therefore the original lithological column of the piston core should reconstruct 155 cm long as following simple calculation; 270 cm (total recovered length) - 127 cm (flow-in section) + 12 cm (the surface oxidized layer). The depth of the piston core is described as cm-below-sea-floor (cm-bsf) based on the original lithological column.

The piston core sediments are predominantly olive black (7.5Y3/2) silty clay including many volcanic glasses as hemipelagic clayey sediments. Two gray (7.5Y4/1 and 5/1) volcanic ash layers are seen at 12 - 13 cm-bsf and 80-84 cm-bsf. The former ash layer is high magnetic susceptibility of 6 x 10^{-3} SI, whereas the latter ash layer is low magnetic susceptibility of 1 x 10^{-3} SI. That of the silty clay is about 2 x 10^{-3} SI. Shear strength increases successively about 15 kPa at about 100 cm-bsf, whereas it decreases to 10 kPa with increasing depth.

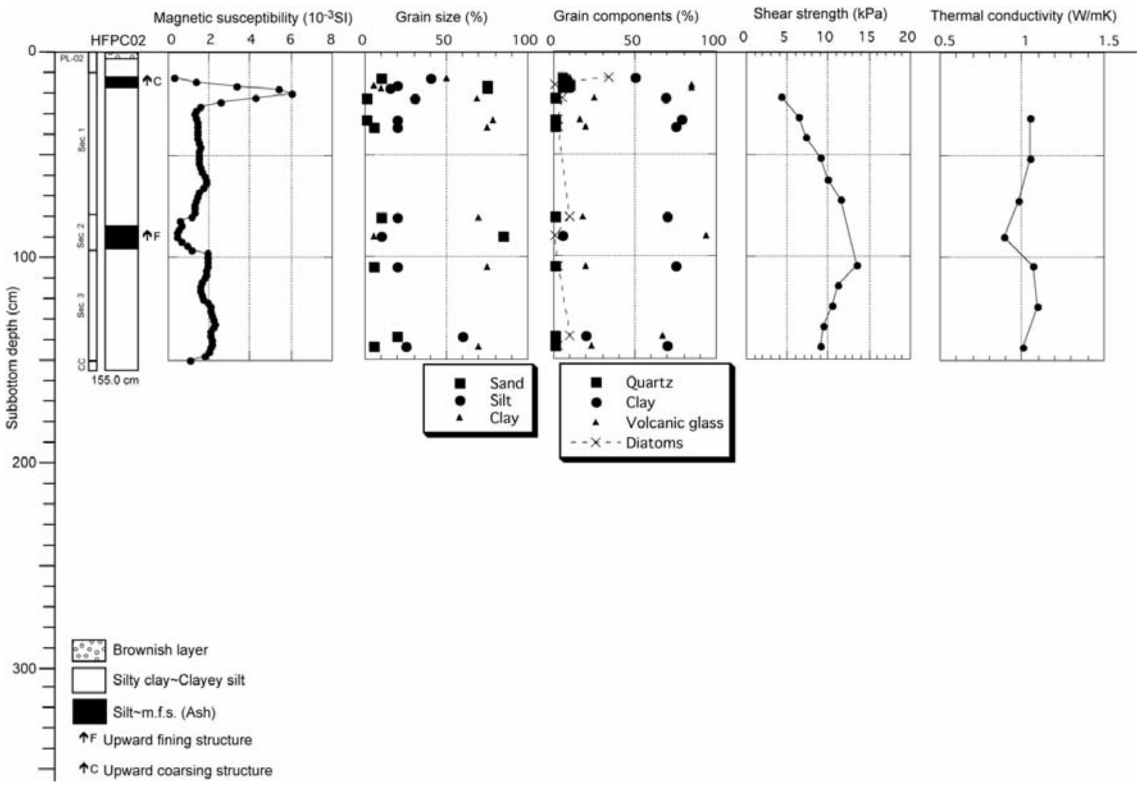

Figure 3.5-6. HFPC02.

[HFPC03 and HFPL03]

To measure the heat flow along the previous multi-channel survey line of 40°15’, HFPC03 was conducted on a westward gentle slope on a horst at 40°15.03’N and 144°57.99’E. The water depth was 5815 m. At this coring site, the subbottom profile image was transparent.

The piston and pilot cores are 155 and 98.5 cm long, respectively (Fig. 3.5-7). But the pilot core penetrated probably twice into the seabed, because a surface oxidized layer can be seen at 14 - 15 cm in depth. This horizon is probably the topmost of the second penetration. Above the oxidized layer, the sediments are olive black clayey silt, which is similar to the sediments around 30 cm deep of the pilot core. This may indicate that these sediments from 0 to 14 cm in depth are the lower part of the first penetration.

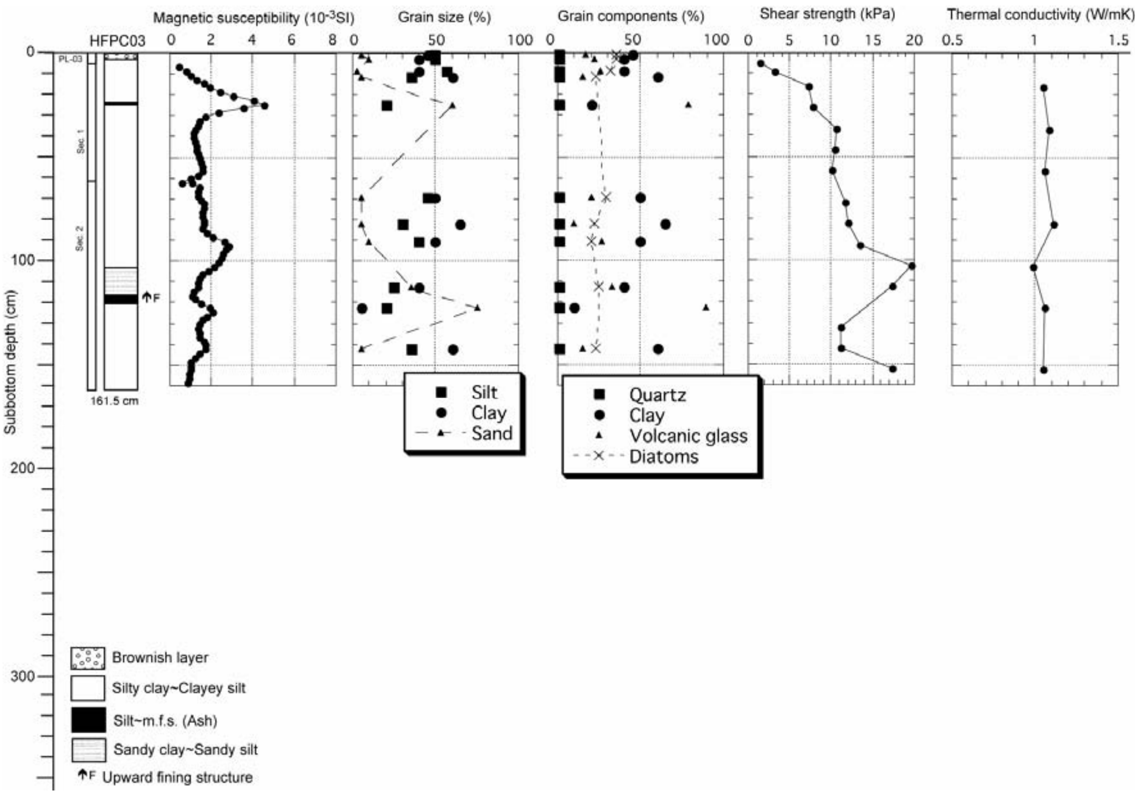

Figure 3.5-7. HFPC03.

The upper part of the piston core should reconstruct as following reasons. Below the oxidized layer in the pilot core, very soft sediments are seen from 15 to 24 cm in depth. These very soft sediments are also seen from 0 to 3.5 cm in Section 1 of the piston core HFPC03. In short, the thickness of the very soft sediments in the pilot core is 9 cm, whereas that of the piston core is 3.5 cm. This indicates that the very soft sediments in the piston core were lost about 5.5 cm, and the surface oxidized layer of 1 cm thickness was lost from the piston core. Therefore the piston core needs to add the surface sediments of about 6.5 cm in thickness, and the original length of the piston core should be 161.5 cm (6.5 cm + 155 cm). The depth of the piston core is described as cm-below-sea-floor (cm-bsf) based on the original length.

The major lithology of the HFPC03 is olive black (10Y3/2) silty clay with diatoms. Two volcanic ash layers are seen at 24.5 - 26.5 and 118.5 - 126.5 cm-bsf. A rounded pebble-sized mudstone is at 51.5 cm-bsf, which is probably a drop stone. Magnetic susceptibility pattern of this core is mostly similar to those of the HFPC01 and 02. Shear strength increases progressively from about 0 to about 20 kPa with increasing depth, because of burial consolidation of the sediments.

[HFPC04 and HFPL04]

To measure the heat flow along the previous multi-channel survey line of 40°15’, HFPC04 was conducted on an edge of a fore-arc basin on a landward slope at 40°15.02’N and 143°03.50’E. The water depth was 1425 m. At this coring site, the subbottom profile image shows parallel layers.

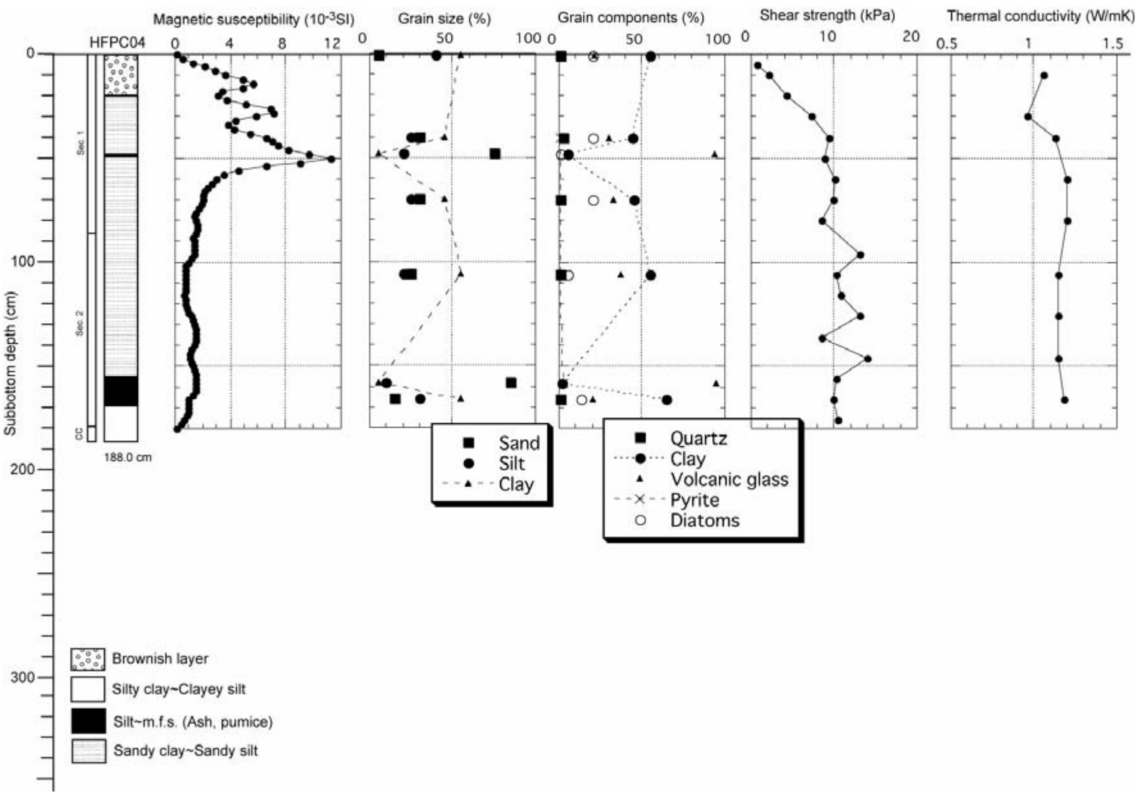

Figure 3.5-8. HFPC04.

The piston and pilot cores are 188 cm long and 40.5 cm long, respectively (Fig. 3.5-8). The core sediment is predominantly olive black (7.5Y3/2) sandy clay with diatoms. The sediments contain many volcanic glasses. Two pumiceous volcanic ash layers are seen at 47 -

49 and 156 - 164 cm-bsf. Magnetic susceptibility has three peaks at about 10, 30 and 50 cm-bsf, and shear strength increases rapidly from about 0 to about 10 kPa at around 50 cm-bsf. It is about 10 kPa from around 50 to 188 cm-bsf.

[HFPC05 and HFPL05]

To measure the heat flow along the previous multi-channel survey line of 40°15', HFPC05 was conducted on a mid-slope terrace on a landward slope at 40°14.94'N and 143°42.29'E. The water depth was 2890 m. At this coring site, the subbottom profile image shows parallel layers.

The piston and pilot cores are 234 cm long and 54 cm long, respectively (Fig. 3.5-9). The core sediment is predominantly olive black (7.5Y3/2-10Y3/2) silty clay with diatoms. The sediments contain many volcanic glasses. A gray (5Y4/1) volcanic ash layer is seen at 58 - 60 cm-bsf. A drop stone of a rounded pebble-sized rock (gabbro?) is seen at 197.5 cm-bsf. Magnetic susceptibility has one peaks at around 60 cm-bsf which is correspondent with the volcanic ash layer. Shear strength increases rapidly from about 0 to about 25 kPa at around 130 cm-bsf. It is constantly about 25 kPa from around 130 to 230 cm-bsf.

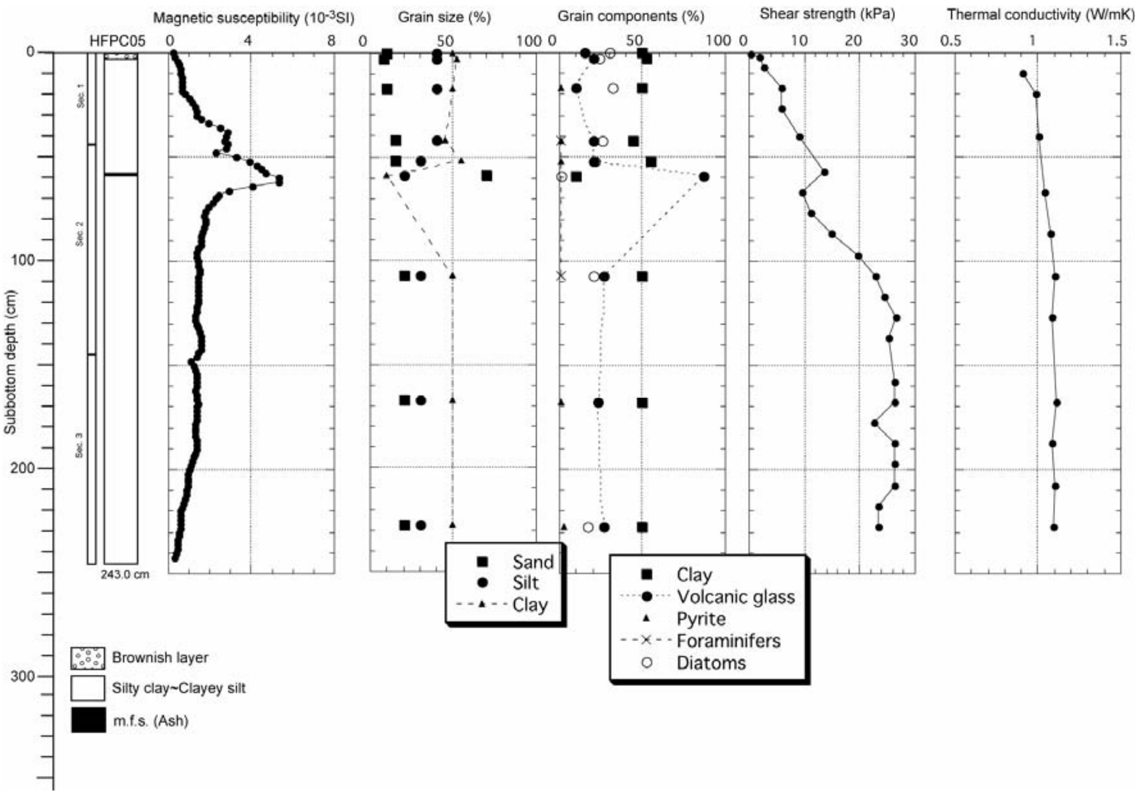

Figure 3.5-9. HFPC05.

[HFPC06 and HFPL06]

To measure heat flow at the upper landward slope in the Japan Trench, HFPC06 was conducted at the gentle slope of 39°14.99'N and 142°51.07'E. The water depth was 1700 m.

The piston core and pilot core are 254 and 54 cm long, respectively (Fig. 3.5-10). The piston core is composed of predominantly olive black (7.5Y3/2~10Y3/2) silty clay with diatoms. The sediments contain many volcanic glasses throughout the core. Two volcanic ash layers are seen at 80 - 86 and 230 - 233 cm-bsf. At 185 - 230 cm-bsf, the core sediments are sandy clay with forams and/or diatoms. In the sandy clay, upward fining structures are seen at 185 - 199, 199 - 217, and 217 - 230 cm-bsf. The magnetic susceptibility is smaller than 5 x 10^{-4} SI in the silty clay, but it is larger than 2 x 10^{-3} SI in the volcanic ash layers. Shear strengths increase progressively from about 0 to 20 kPa throughout the core.

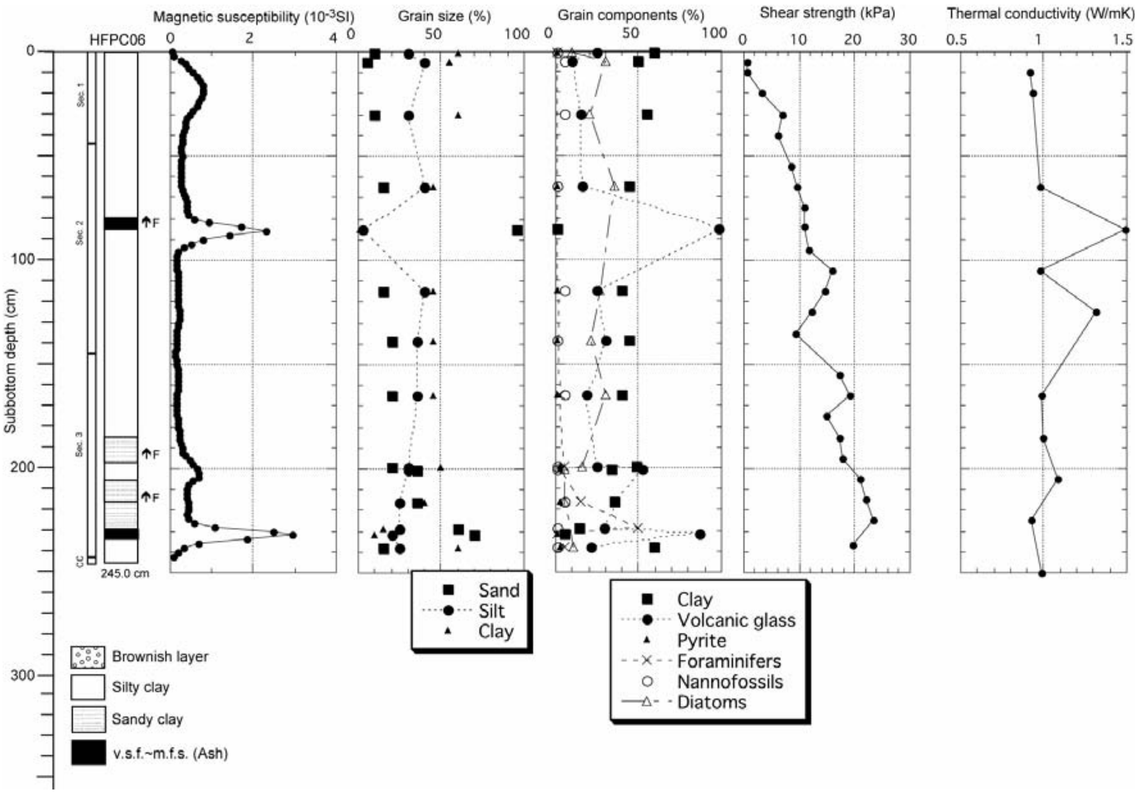

Figure 3.5-10. HFPC06.

[7K#430 C-1]

To measure thermal and electric conductivities, this core was collected from the flat mud surface near the OBE site (40°14.89'N, 145°41.22'E) using a MBARI corer of KAIKO 7000II. The water depth was 5210 m. The coring site was approximately 5 m west from the SAHF measurement point.

This core is 26.5 cm long (Fig. 3.5-11). It is composed of mainly olive gray (10Y4/2) silty clay with diatoms. A surface oxidized layer of dark olive (5Y4/3) silty clay with diatoms is at 0 - 0.5 cm in depth. Pyritized burrows are seen at 8 - 10, 11 - 21 and 23 - 24 cm in depth.

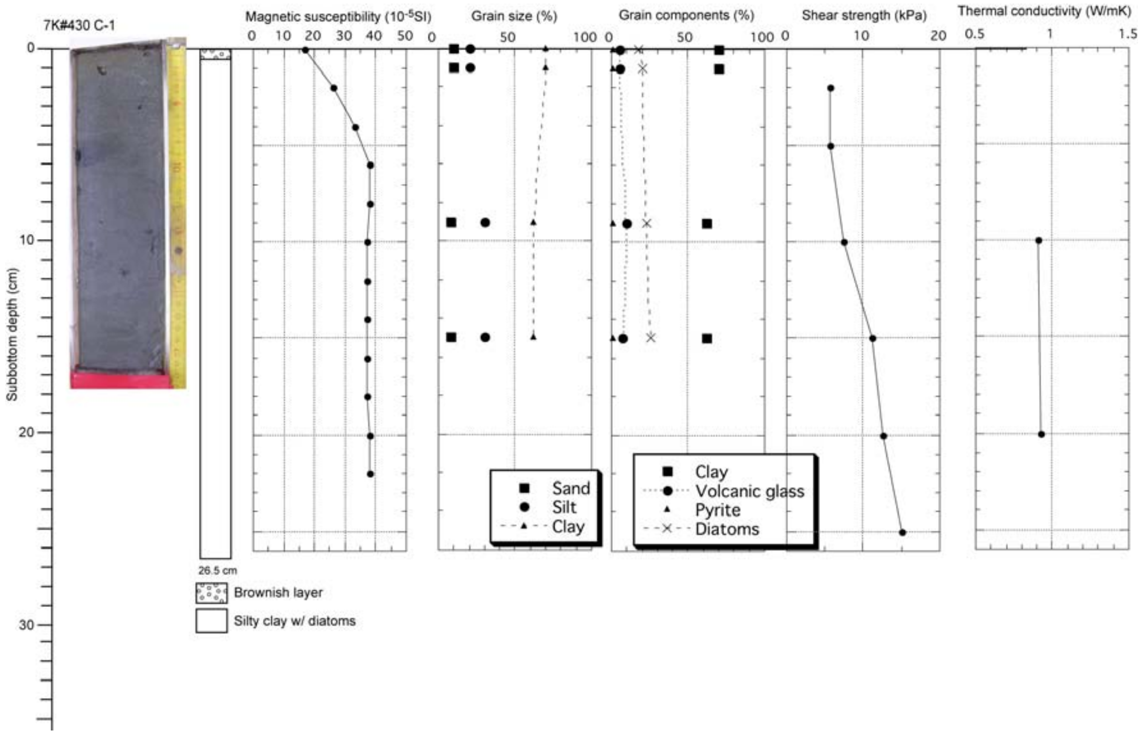

Figure 3.5-11. 7K#430 C-1.

3.5.4. Deployment of LT-OBEMs

We first mapped the bathymetry in the vicinity of planned position using SeaBeam system and select flat seafloor for the final deployment point (Fig. 3.5-12). The LT-OBEMs were launched from deck using A-frame and sunk by their self weights. The operations were quick and smooth. We tracked the LT-OBEMs by acoustic signals and confirmed that the LT-OBEMs were successfully settled on the seafloor. Then, the settled positions were determined by measurements of the slant ranges at least three positions surrounding the launching point for TT4 at site L01 and by Super Short Base Line (SSBL) positioning system of R/V KAIREI for TT1 at site L02 (Fig. 3.5-13). The information that will be needed for the recovery and the data analysis are listed in Table 3.5-4.

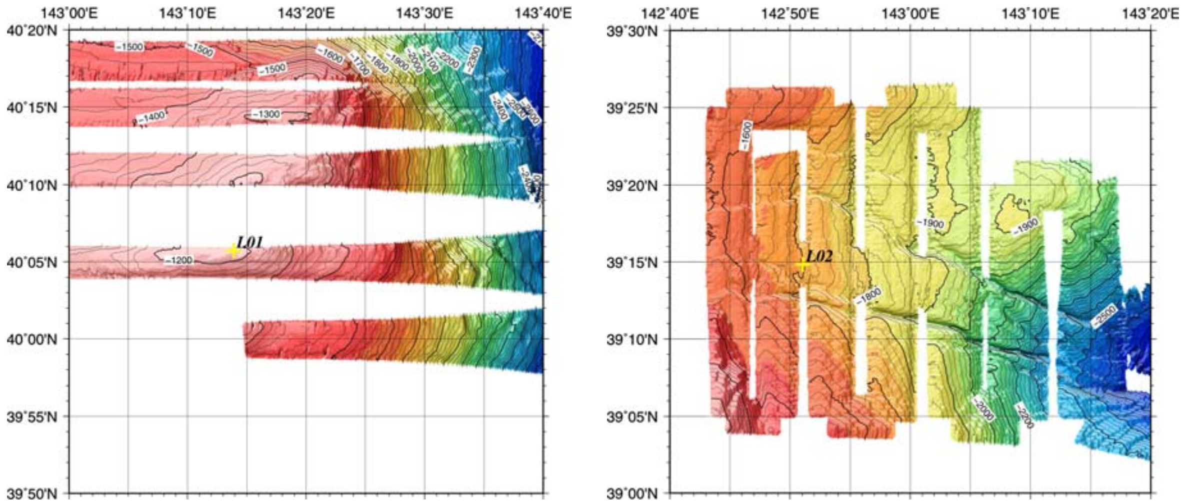

Figure 3.5-12. Bathymetric map and site location for sites L01 (left) and L02 (right).

Table 3.5-4. Information of the LT-OBEMs.

Site	L01	L02
OBEM ID	TT4	TT1
Launched position	40° 05.576' N 143° 13.849' E	39° 14.942' N 142° 51.275' E
Settled position	40° 05.733' N 143° 13.897' E	39° 14.832' N 142° 51.069' E
Depth	1230 m	1686 m
sampling intervals	60 s	60 s
Dipole length (N-S)	5.24 m	5.41 m
Dipole length (E-W)	5.22 m	5.41 m
Time for clock reset to GPS (TZ = ±0h)	2008-09-05 00:51:00	2008-09-07 09:38:01
Time for recording start (TZ = ±0h)	2008-09-09 14:58:00	2008-09-12 14:58:00
Acoustic system	Benthos	Kaiyo Denshi
frequency (Tx, ship side)	10.0 kHz	9.494 kHz
frequency (Rx, ship side)	11.0 kHz	13.499 kHz
Release command	C	4A-1
Radio beacon	Taiyo musen	Taiyo musen
frequency	43.528 MHz	43.528 MHz
ID	JS1086	JS190
Flash light	Taiyo musen	Taiyo musen

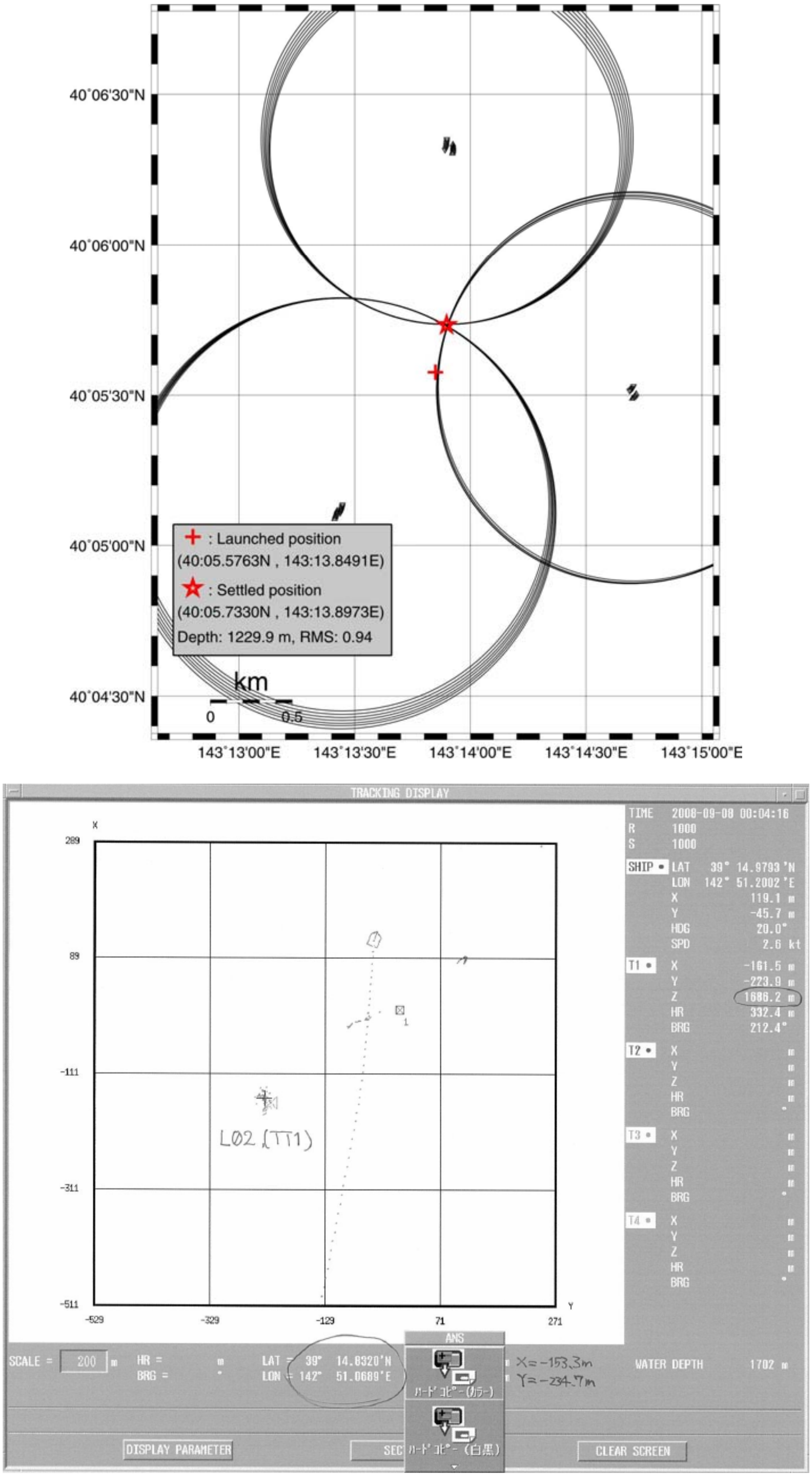

Figure 3.5-13. Determination of the position LT-OBEM on the seafloor. Top is for TT4 at L01 and bottom is for TT1 at L02, respectively.

3.5.5. HF-OBEM and CSEM experiment

Two HF-OBEs and one HF-OBEM were deployed along the 40°15'N survey line on the seaward side of the Japan Trench during the Leg 1. They were successfully recovered during the Leg 2 (Table 3.5-5).

The ROV KAIKO 7000I dived to the OBE as shown in the following photos (Fig. 3.5-14). The CSEM signal shot from the ROV was successfully recorded by the OBE. However, the CSEM transmitter had some trouble, and the term of CSEM shooting was so limited (within a few seconds). The obtained data is shown in Fig. 3.5-15.

Table 3.5-5. Deployment and recovery of the HF-OBEMs.

Site No.	Instrument	Deployment		Descending	Landing		Release (Time in JST)			Ascending
		Time (JST)	Ship's Position	Speed	Time(JST)	Position (SSBL	Command	Launching	Surface	Speed
101	OBEM (TIT101)	2008/8/20 15:29	40-15.0552' N 145-01.9804' E W.D .= 5763 m	47 m/min	2008/8/20 17:33	40-14.6577' N 145-02.1998' E W.D. = 5730 m	2008/9/3 03:43	2008/9/3 03:57	2008/9/3 06:06	45 m/min
102	OBE (JF2)	2008/8/23 18:10	40-15.0074' N 145-25.0076' E W.D. = 5396 m	47 m/min	2008/8/23 20:04	40-14.7338' N 145-24.9464' E W.D. = 5426 m	2008/9/4 03:49	2008/9/4 04:06	2008/9/4 05:43	55 m/min
103	OBE (JF1)	2008/8/20 05:57	40-14.9930' N 145-41.0191' E W.D. = 5222 m	47 m/min	Not monitored	40-14.9719' N 145-41.2412' E W.D. = 5220 m	2008/9/4 14:33	2008/9/4 14:50	2008/9/4 16:29	53 m/min

cf. The landing point at site 103 should be modified as follows, because
the ship position is far from the OBE (about 1000m in horizontal distance
40-14.9452' N
145-41.2224' E

Figure 3.5-14. (a) ROV KAIKO 7000II.

Figure 3.5-14. (b) Camera images obtained by KAIKO.

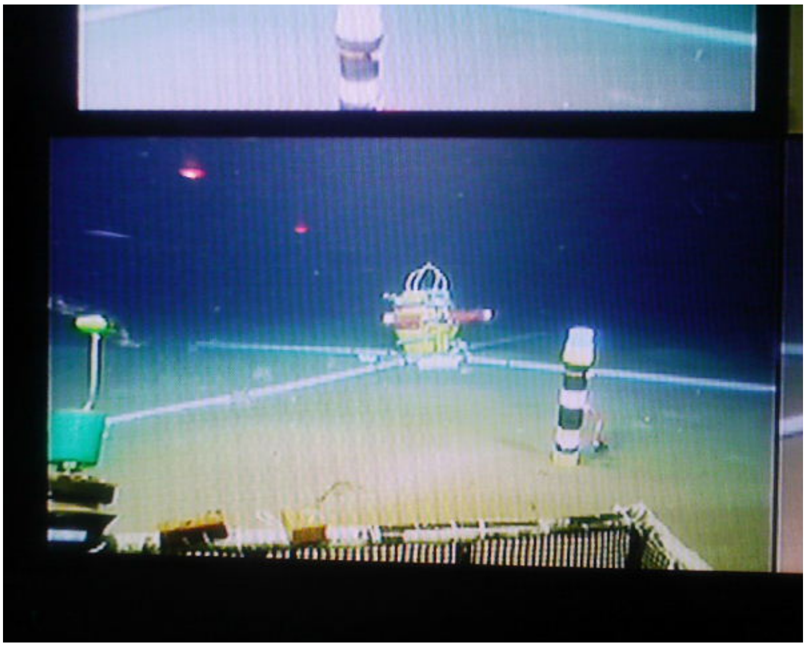

(c) OBE captured by the KAIKO camera.

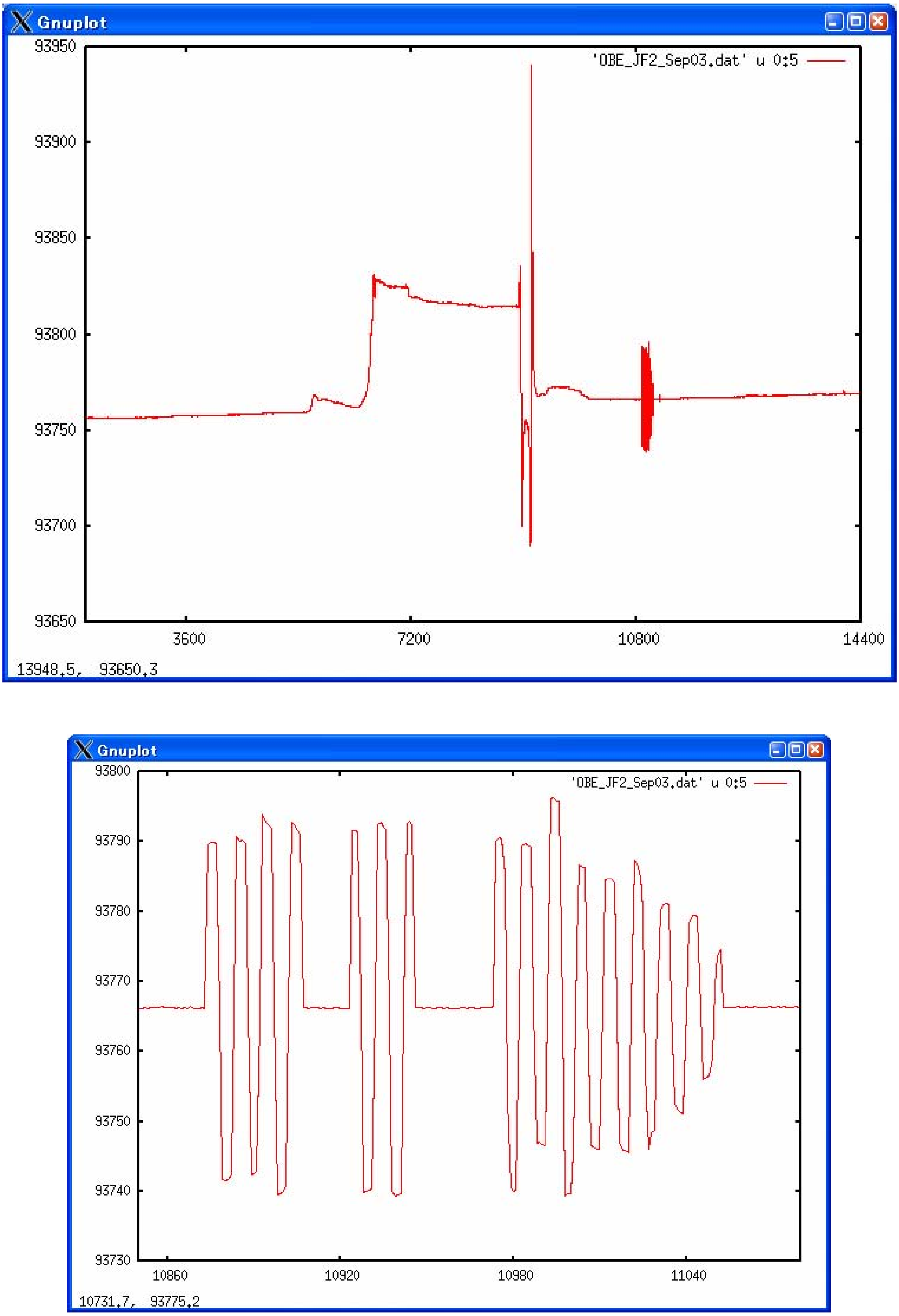

Figure 3.5-15. Upper: Electric time series recorded by OBE (JF2) between E-electrode and GND-electrode. Lower: Enlargement of recorded signal.

3.5.6. Bathymetry and geophysical survey

Bathymetry and geophysical mapping surveys were made mainly at night in the vicinity of the 40°15'N line and around 39°N. The surveyed lines are listed in the Appendices (7.2). On all the lines, measurements of gravity and three components of the geomagnetic field were conducted with instruments on board as well as bathymetry mapping with a SeaBeam system. The total intensity of the geomagnetic field was measured with a proton precession magnetometer along some selected ENE-WSW lines on the seaward side of the Japan Trench (cf. 7.2). We also made 3.5 kHz subbottom profiling (SBP survey in 7.1) around piston coring sites for imaging structures in surface sediments.

4. Notice on Using

This cruise report is a preliminary documentation as of the end of the cruise. It may not be corrected even if changes on content (i.e. taxonomic classifications) are found after publication. It may also be changed without notice. Data on the cruise report may be raw or not processed. Please ask the Chief Scientist for the latest information before using.

Users of data or results of this cruise are requested to submit their results to Data Integration and Analysis Group (DIAG), JAMSTEC.

5. Acknowledgements

We are grateful to Captain E. Ukekura, the officers and the crew of the R/V KAIREI, ROV Operation Manager K. Hirata, and the operation team of the ROV KAIKO 7000II for skillful operations of the ship, ROV, and research equipment. We also extend our thanks to S. Minamizawa, E. Hatakeyama, N. Togashi, and A. So for giving us great assistance in research works throughout the cruise. The staff of the Operation Group, Research Vessel Operation Department, Marine Technology Center, especially T. Hirai, made excellent arrangements for the cruise.

The research conducted on this cruise was partly supported by Japan Society for the Promotion of Science through a Grant-in Aid for Scientific Research (19340125).

6. References

Fujie, G., J. Kasahara, R. Hino, T. Sato, M. Shinohara, and K. Suyehiro, A significant relation between seismic activities and reflection intensities in the Japan Trench region, Geophys. Res. Lett., 29, 7, 10.1029/20, 2002.

Goto, T., H. Mikada, K. Suyehiro, K. Yamane, L. Lewis, A. Orange, E. Nichols, and S. Constable, Electrical conductivity structures across seismically active and less active zones on the subducting Pacific plate, off northeast Japan, Eos Trans. AGU, 82(47), Fall Meet. Suppl.: Abstract GP21A-0249, 2001.

Hamamoto, H., M. Yamano, and S. Goto, S., Heat flow measurement in shallow seas through long-term temperature monitoring, Geophys. Res. Lett., 32, L21311, doi:10.1029/2005GL024138, 2005.

Hirano N, K. Kawamura, M. Hattori, K. Saito, and Y. Ogawa, A new type of intra-plate volcanism; young alkali-basalts discovered from the subducting Pacific Plate, northern Japan Trench, Geophys. Res. Lett., 28, 2719-2722, 2001.

Hirano N, E. Takahashi, J. Yamamoto, N. Abe, S.P. Ingle, I. Kaneoka, T. Hirata, J. Kimura, T. Ishii, Y. Ogawa, S. Machida, and K. Suyehiro, Volcanism in response to plate flexure, Science, 313, 1426-1428, 2006.

Ito, A., G. Fujie, T. Tsuru, S. Kodaira, A. Nakanishi, and Y. Kaneda, Fault plane geometry in the source region of the 1994 Sanriku-oki earthquake, Earth Planet. Sci. Lett., 223, 163-175, 2004

Oleskevich, D.A., R.D. Hyndman, and K. Wang,, The updip and downdip limits to great subduction eartquakes: thermal and structural models of Cascadia, south Alaska, SW Japan, and Chile, J. Geophys. Res., 104, 14965-14991, 1999.

Nakajima, J., and A. Hasegawa, Anomalous low-velocity zone and linear alignment of seismicity along it in the subducted Pacific slab beneath Kanto, Japan: Reactivation of subducted fracture zone?, Geophys. Res. Lett., 33, doi:10.1029/2006GL026773, 2006.

Sass, J.H., C. Stone, and R.J. Munroe, Thermal conductivity determinations on solid rocks - a comparison between a steady-state divided-bar apparatus and a commercial transient line-source device, Jour. Volcanol. Geotherm. Res., 20, 145-153, 1984.

Tsuru, T, J.-O. Park, N. Takahashi, S. Kodaira, Y. Kido, Y. Kaneda, and Y. Kono, Tectonic features of the Japan Trench convergent margin off Sanriku, northeastern Japan, revealed by multichannel seismic reflection data, J. Geophys. Res., 105, 16,403-16,413, 2000.

Von Herzen, R., and A.E. Maxwell, The measurement of thermal conductivity of deep-sea sediments by a needle-probe method, J. Geophys. Res., 64, 1557-1563, 1959.

Yamano, M., M. Kinoshita, and S. Goto, High heat flow anomalies on an old oceanic plate observed seaward of the Japan Trench, Int. J. Earth. Sci, 97, 345-352, 2008.

Yamanaka, Y., and M. Kikuchi, Asperity map along the subduction zone in northeastern Japan inferred from regional seismic data, J. Geophys. Res., 109, B07307, doi:10.1029/2003JB002683, 2004.

7. Appendices

7-1. Cruise Log

KR08-10 Shipboard Log 1/3				Position/Weather/ Wind/Sea condition (Noon)
Date	Time	Description	Remarks	
18Aug08	9:30	Scietists embark on Kairei		12:00(GMT+9h)
	10:00	Leave the YOKOSUKA port for research area	Head for Japan Trench	34-58.5N, 139-39.6E
	11:00-11:30	Carried out onboard education & training for scientists		Fine but Cloudy
	11:30-12:00	Scientific meeting		NNW-3 (Gentle breeze)
	13:00-13:30	Cruise Meeting		Sea slight
	16:40-17:00	Konpira ceremony		
19Aug08	12:15	Arrived at research area	Japan Trench	12:00(GMT+9h)
	12:24	Released XBT	at 40-07.7549N,144-24.7809E	40-04.8N, 140-22.0E
	13:34	Com'ced towing proton magnetmeter, MBES mapping survey, SBP survey		Overcast
	18:00-18:15	Scientific meeting		ESE-5 (Fresh breeze)
	20:00	Finished SBP survey		Sea slight
20Aug08	4:58	Finished MBES mapping survey		12:00(GMT+9h)
	5:36	Recovered proton magnetmeter		40-15.0N, 145-39.7E
	5:57	Deployed OBE at 40-14.9930N, 145-41.0191E, D=5222n	Landed at 40-14.9719N, 145-41.2412E, D=5220	Overcast
	06:54-13:07	Carried out heat flow sampling (HF01)		North-5 (Fresh breeze)
	12:05-12:11	Carried out SSBL calibration		Sea slight
	15:28	Deployed OBEM at 40-15.0552N, 145-01.9804E, D=5763m		
	17:36-17:42	Carried out SSBL calibration		
	17:42	Fixed OBEM	Landed at 40-14.6577N, 145-02.1998E, D=5730m	
	18:00-18:20	Scientific meeting		
	18:50	Com'ced MBES mapping survey & SBP survey		
	20:00	Finished SBP survey		
21Aug08	4:00	Finished MBES mapping survey		12:00(GMT+9h)
	5:30	Arrived at HFPC point		40-15.0N, 146-26.5E
	6:19-11:02	Carried out heat flow PC sampling (HFPC01)		Overcast
	12:37-17:35	Carried out heat flow sampling (HF02)		NE-6 (Strong breeze)
	17:44	Com'ced towing proton magnetmeter		Sea moderate
	18:24	Com'ced MBES mapping survey		
	19:00-19:25	Scientific meeting		
22Aug08	2:45	Finished MBES mapping survey		12:00(GMT+9h)
	5:35	Recovered proton magnetmeter		40-15.0N, 145-16.8E
	6:02-11:20	Carried out heat flow sampling (HF03)		Fine but Cloudy
	12:52-18:00	Carried out heat flow sampling (HF04)		NNE-6 (Strong breeze)
	18:05	Com'ced towing proton magnetmeter		Sea moderate
	19:15-19:40	Scientific meeting		
	19:38	Com'ced MBES mapping survey		
23Aug08	4:35	Finished MBES mapping survey		12:00(GMT+9h)
	5:30	Recovered proton magnetmeter		40-15.0N, 145-14.0E
	5:48-10:10	Carried out heat flow PC sampling (HFPC02)		Fine but Cloudy
	11:17-17:14	Carried out heat flow sampling (HF05)		ENE-3 (Gentle breeze)
	18:10	Deployed OBE at 40-14.9930N, 145-25.0076E, D=5396n	Landed at 40-14.7338N, 145-24.9464E, D=5426	Sea slight
	18:35-18:48	Scientific meeting		
24Aug08	1:40-4:11	Carried out MBES mapping survey		12:00(GMT+9h)
	6:06-6:13	Carried out SBP survey		39-18.0E, 142-55.7E
	6:26-10:44	Carried out heat flow sampling (HF06)		Overcast
	12:40	Arrived at abore point		East-6 (Strong breeze)
	12:45-14:45	Carried out PHF calibration (PHF01)		Sea moderate
	15:00	Left research area for off MIYAKO due to overd rough se	Head for MIYAKO	
	18:30	Let go her aunchor in 15m of water		
	18:00-18:15	Scientific meeting		
25Aug08				12:00(GMT+9h)
				39-37.9N, 141-58.9E
				Overcast
				NNE-2 (Light breeze)
				Sea calm (Rippled)
26Aug08	5:00	Com'ced proceeding to research area	Head for Japan Trench	12:00(GMT+9h)
	8:00	Arrived at research area		39-14.0N, 142-58.5E
	8:07-9:32	Carried out MBES mapping survey & SBP survey		Overcast
	9:54-12:22	Carried out heat flow sampling (HF07)		NE-5 (Fresh breeze)
	13:32-15:14	Deployed PHF01 (D=1830m)	at 39-14.02N, 142-58.50E	Sea moderate
	15:57	Deployed PWT01 (D=1710m)	at 39-14.9149Nm 142-51.2320E	
	16:06-18:00	Carried out above PHF02 calibration		
	18:06	Com'ced shifting to HFPC03 point		
	19:00-19:30	Scientific meeting		

KR08-10 Shipboard Log 2/3				Position/Weather/
Date	Time	Description	Remarks	Wind/Sea condition
27Aug08	3:30	Arrived at HFPC03 point & com'ced drifting		12:00(GMT+9h)
	5:59-10:30	Carried out heat flow PC sampling (HFPC03)		40-15.0N, 144-43.3E
	11:50-17:55	Carried out heat flow sampling (HF08)		Overcast
	18:00	Com'ced towing proton magnetmeter		ESE-5 (Fresh breeze)
	19:00-19:18	Scientific meeting		Sea slight
	20:23	Com'ced MBES mapping survey		
28Aug08	4:34	Finished MBES mapping survey		12:00(GMT+9h)
	5:33	Recovered proton magnetmeter		40-15.0N, 145-50.0E
	5:59-11:17	Carried out heat flow sampling (HF09)		Cloudy
	12:30-17:57	Carried out heat flow sampling (HF10)		South-4 (Moderate breeze)
	18:04	Com'ced towing proton magnetmeter		Sea slight
	18:30	Com'ced MBES mapping survey		
	19:00-19:10	Scientific meeting		
29Aug08	2:20	Finished MBES mapping survey		12:00(GMT+9h)
	5:36	Recovered proton magnetmeter		40-15.0N, 145-03.0E
	5:57-18:03	Carried out heat flow sampling (HF11)		Cloudy
	18:11	Com'ced MBES mapping survey		SSE-4 (Moderate breeze)
	19:00-19:30	Scientific meeting		Sea slight
30Aug08	5:32	Finished MBES mapping survey		12:00(GMT+9h)
	5:55-6:58	Carried out SBP survey		40-14.9N, 142-58.5E
	7:27-7:56	Carried out PWT02 calibration		Rain
	8:13-12:11	Carried out heat flow sampling (HF12)		NW-2 (Light breeze)
	12:30-14:00	Deployed PHF02 (D=1420m)	at 40-15.07N, 142-58.97E	Sea slight
	14:32-16:33	Carried out heat flow PC sampling (HFPC04)		
	17:22	Carried out MBES mappingsurvey & SBP survey		
	18:30-19:15	Scientific meeting		
	20:00	Finished SBP suevey		
31Aug08	2:33	Finished MBES mapping survey		12:00(GMT+9h)
	6:28	Recovered PWT02 (D=1420m)	at 40-15.05N, 142-59.28E	40-15.0N, 143-43.0E
	7:05	Deployed PWT03 (D=1419m)	at 40-14.9950N, 143-03.5113E,	Rain
	7:32-8:12	Carried out above PWT03 calibration		ENE-4 (Moderate breeze)
	10:02-10:40	Carried out MBES mapping survey		Sea slight
	11:18-16:50	Carried out heat flow sampling (HF13)		
	17:00	Left research area for MIYAKO	Head for MIYAKO	
01Sep08	8:45	Arrived at MIYAKO		The port of MIYAKO
	10:45	One scietist disembark From Kairei		12:00(GMT+9h)
	15:00	Five scientists embark on Kairei		39-38.0N, 141-58.2E
				Cloudy
				NW-3 (Gentle breeze)
				Sea Calm (Rippled)
02Sep08	8:00	Left the MIYAKO port for research area	Head for Japan Trench	12:00(GMT+9h)
	8:35-9:10	Carried out onboard education & training for scientists		39-40.0N, 143-00.0E
	9:10-10:00	Scientific meeting		Cloudy
	11:00	Aeeived at research area		SE-4 (Moderate breeze)
	13:18	Hoisted up "KAIKO 7000Ⅱ"		Sea slight
	13:24	Launched "KAIKO 7000Ⅱ" dove & started her operation	Dive#428	
	15:32	Hoisted up "KAIKO 7000Ⅱ"		
	15:44	Finished above operation		
	16:09	Com'ced proceeding to OBEM point		
	18:00-18:30	Scientific meeting		
03Sep08	6:19	Recovered OBEM		12:00(GMT+9h)
	7:30	Released XBT	at 40-14.4444N, 145-23.7986E	40-14.9N, 145-25.0E
	8:27	Hoisted up "KAIKO 7000Ⅱ"	Dive#429	Cloudy
	8:34	Launched "KAIKO 7000Ⅱ" dove & started her operation		SSE-4(Moderate breeze)
	10:50	Landed on the sea bottom (D=5390)		Sea smooth
	14:16	"KAIKO 7000Ⅱ" left the sea bottom (D=5390m)		
	16:01	Hoisted up "KAIKO 7000Ⅱ"		
	16:11	Finished above her operation		
	16:40	Com'ced proseeding to MBES mapping survey point		
	18:00-18:30	Scientific meeting		

KR08-10 Shipboard Log 3/3				Position/Weather/
Date	**Time**	**Description**	**Remarks**	**Wind/Sea condition**
04Sep08	1:11	Finished MBES mapping survey		12:00(GMT+9h)
	5:50	Recovered OBE		40-15.0N, 145-41.3E
	8:18	Hoisted up "KAIKO 7000Ⅱ"	Dive#430	Fine but Cloudy
	8:25	Launched "KAIKO 7000Ⅱ" dove & started her operation		NNW-3 (Gentle breeze)
	11:08	Landed on the sea bottom (D=5207m)		Sea smooth
	13:14	"KAIKO 7000Ⅱ" left the sea bottom (D=5207m)		
	14:55	Hoisted up "KAIKO 7000Ⅱ"		
	15:03	Finished above her operation		
	16:35	Recovered OBE		
	16:40	Com'ced proseeding to MBES mapping survey point		
	18:00-18:30	Scientific meeting		
	18:30	Com'ced MBES mapping survey		
05Sep08	2:41	Finished MBES mapping survey & proceeded to MIYAKO	Head for MIYAKO	12:00(GMT+9h)
	6:50	Let go her aunchor in 21m off depth at off MIYAKO		39-54.0N, 142-41.6E
	9:30	Hove up aunchor & com'ced proceeding to research area	Head for Japan Trench	Overcast
	11:00	Arrived at research area		NW-3 (Gentle breeze)
	14:06	Deployed OBEM		Sea smooth
	14:15-15:50	Carried out above calibration	Landed at 40-05.7156N, 143-13.9032E, D=1205m	
	16:21-18:52	Carried out MBES mapping survey		
	18:00-19:05	Scientific meeting		
06Sep08	5:58-8:49	Carried out heat flow PC sampling (HFPC05)		12:00(GMT+9h)
	8:55-10:25	Carried out MBES mapping survey & SBP survey		40-15.0N, 144-00.5E
	10:57-17:00	Carried out heat flow sampling (HF14)		Fine but Cloudy
	19:18-22:25	Carried out MBES mapping survey		East-3 (Gentle breeze)
				Sea smooth
07Sep08	6:59-16:52	Carried out heat flow sampling (HF15)		12:00(GMT+9h)
	16:55	Com'ced shifting to SW ward	Head for OBEM deploying point	40-15.0N, 145-40.6E
	18:00-18:30	Scientific meeting		Fine but Cloudy
				NE-3 (Gentle breeze)
				Sea smooth
08Sep08	5:30-6:15	Shifted to NNE ward		12:00(GMT+9h)
	8:00	Deployed OBEM		39-17.1N, 142-50.6E
	8:16-8:49	Carried out PWT01 calibration		Fine but Cloudy
	9:00	Carried out OBEM calibration		North-4 (Moderate breeze)
	9:27-11:39	Carried out heat flow PC sampling (HFPC06)		Sea smooth
	12:30	Com'ced MBES mapping survey		
09Sep08	5:06	Finished MBES mapping survey		12:00(GMT+9h)
	5:57-6:15	Carried out MBES & SBP mapping survey		39-05.1N, 143-40.0E
	6:37-10:13	Carried out heat flow sampling (HF16)		Fine but Cloudy
	10:43-11:35	Carried out MBES & SBP mapping survey		NNW-6 (Strong breeze)
	11:35	Left research area for Yokosuka	Head for Yokosuka	Sea rough
10Sep08	8:30-10:20	Ship tour	Head for Yokosuka	12:00(GMT+9h)
	17:00	Arrived at YOKOSUKA		34-58.3N, 139-43.6E
	18:00	Scietists disembark From Kairei		Fine but Cloudy
				ENE-5 (Fresh breeze)
				Sea slight

7-2. Bathymetry Survey Lines

Line Name	Start date	Time(UTC)	Latitude	Longitude	End date	Time(UTC)	Latitude	Longitude	Remark
0819 Line1	8/19	04:34	40-15.0576N	144-29.9120E	8/19	14:03	40-26.0142N	147-03.0004E	proton magnetmeter
0819 Line2	8/19	15:06	40-37.9203N	146-56.7388E	8/19	19:58	40-14.9855N	145-47.9886E	proton magnetmeter
0820 Line1	8/20	09:50	40-19.0636N	145-15.0668E	8/20	11:19	40-18.8034N	144-49.8208E	
0820 Line2	8/20	11:54	40-11.1309N	144-50.2982E	8/20	19:00	40-11.0046N	146-34.9328E	
0821 Line1	8/21	09:24	40-21.9738N	146-29.8489E	8/21	11:28	40-31.7348N	147-00.1630E	proton magnetmeter
0821 Line2	8/21	12:39	40-17.8694N	147-04.7502E	8/21	17:45	39-54.7966N	145-51.3607E	proton magnetmeter
0822 Line1	8/22	10:38	39-59.9570N	145-23.8953E	8/22	15:14	40-22.0423N	146-30.0514E	proton magnetmeter
0822 Line2	8/22	15:19	40-22.9740N	146-29.8090E	8/22	19:35	40-22.9899N	145-18.3259E	proton magnetmeter
0823 Line1	8/23	16:40	39-06.9953N	144-05.0127E	8/23	19:11	39-11.5065N	143-19.9693E	
0825 Line1	8/25	23:07	39-15.6063N	142-44.9777E	8/26	00:32	39-13.5048N	143-01.6982E	
0827 Line1	8/27	11:23	39-41.8452N	144-50.9701E	8/27	17:42	40-09.0184N	146-11.9953E	proton magnetmeter
0827 Line2	8/27	17:51	40-08.9595N	146-11.8859E	8/27	19:34	40-08.9963N	145-49.8851E	proton magnetmeter
0828 Line1	8/28	09:30	40-15.0011N	145-47.0288E	8/28	12:52	39-56.2391N	144-51.9260E	proton magnetmeter
0828 Line2	8/28	13:51	40-08.8334N	144-50.3269E	8/28	17:20	40-08.9980N	145-45.4037E	proton magnetmeter
0829 Line1-1	8/29	10:13	40-08.9749N	145-14.9899E	8/29	18:17	40-15.0025N	143-13.1828E	
0829 Line1-2	8/29	20:10	40-14.9910N	143-13.6669E	8/29	20:32	40-14.9966N	143-08.9182E	
0829 Line2	8/29	20:55	40-14.9929N	143-09.0509E	8/29	21:58	40-14.9993N	142-54.0390E	
0830 Line1	8/30	08:22	40-18.1535N	142-56.5043E	8/30	12:46	40-17.7999N	144-09.9294E	
0830 Line2	8/30	13:22	40-10.9975N	144-09.5504E	8/30	17:33	40-11.0009N	142-59.9647E	
0831 Line1	8/31	01:02	40-15.0184N	143-39.9986E	8/31	01:40	40-14.9992N	143-50.1373E	
0908Line1	9/8	03:30	39-22.0525N	142-48.9729E	9/8	04:43	39-04.9857N	142-48.9896E	
0908Line2	9/8	04:49	39-05.0151N	142-49.0158E	9/8	05:03	39-04.9925N	142-44.9832E	
0908Line3	9/8	05:09	39-04.9851N	142-44.9880E	9/8	06:42	39-25.0052N	142-44.9952E	
0908Line4	9/8	06:48	39-25.0175N	142-44.9859E	9/8	07:20	39-25.0026N	142-53.5728E	
0908Line5	9/8	07:28	39-25.0250N	142-53.4855E	9/8	09:00	39-05.1894N	142-53.4915E	
0908Line6	9/8	09:07	39-04.9972N	142-53.4274E	9/8	09:27	39-04.9972N	142-58.5187E	
0908Line7	9/8	09:33	39-04.8228N	142-58.5104E	9/8	11:12	39-25.0390N	142-58.5009E	
0908Line8	9/8	11:19	39-24.9822N	142-58.4522E	9/8	11:39	39-25.0060N	143-03.7043E	
0908Line9	9/8	11:46	39-25.0199N	143-03.7397E	9/8	13:19	39-04.9636N	143-03.7228E	
0908Line10	9/8	13:24	39-05.0152N	143-03.6679E	9/8	13:44	39-04.9901N	143-08.9291E	
0908Line11	9/8	13:50	39-04.9148N	143-09.0087E	9/8	15:04	39-20.0131N	143-08.8963E	
0908Line12	9/8	15:10	39-20.0220N	143-08.9200E	9/8	15:32	39-19.9963N	143-15.0334E	
0908Line13	9/8	15:38	39-20.0682N	143-14.9927E	9/8	16:47	39-04.9528N	143-15.0032E	
0908Line14	9/8	16:54	39-05.0524N	143-14.9697E	9/8	19:20	38-58.9738N	143-55.1918E	
0908Line15	9/8	19:26	38-58.9659N	143-54.9977E	9/8	20:06	39-07.6007N	143-56.4011E	
0908Line16	9/8	21:02	39-07.6119N	143-55.1083E	9/8	21:15	39-07.5925N	143-57.6059E	
0909Line1	9/9	01:43	39-07.4682N	143-56.4858E	9/9	02:35	39-08.5024N	143-44.9559E	